Fabrication of Nanoparticle Arrays

A project report
submitted in partial fulfillment of the
requirements for the degree of
Master of Engineering
in the Faculty of Engineering

by

Alok Kr. Srivastava

Department of Chemical Engineering,
Indian Institute of Science.

June 2007

Table of Contents

List of Figures

List of Tables

List of Abbreviations

CVD	Chemical Vapour Deposition
MPNs	Moleculary Protected Nanoparticles
TA	Tannic acid
TEM	Transmission Electron Microscopy
AFM	Atomic Force Microscopy
FTIR	Fourier Transform Infrared Spectroscopy
UV-Vis	Ultraviolet-Visible Spectroscopy

Abstract

Gold nanoparticles of different size ranges were synthesized in aqueous medium and subsequently transferred to organic phase after surface functionalization with dodecanethiol. Synthesis condition required to produce monodisperse particles of size range 5nm and 10nm, which are suitable for fabricating ordered arrays were optimized. Fabrication of arrays over water surface under different experimental conditions was investigated. TEM, AFM, UV-Vis and FTIR was used to characterize the arrays formed. Plasma etching was used to remove the capping ligands from ordered nanoparticles. Optimum plasma conditions for both size ranges were obtained such that the ligands are removed without disturbing the lateral ordering of arrays. These gold nanodots could be further utilized as templates for fabricating ordered and addressable nanostructures, essential for harnessing the potential of nanostructures.

Chapter 1: General Introduction

1.1 Introduction

Nanoscience and nanotechnology are two words that have created a lot of excitement in the research community in the recent past. Nanoscience is the study of fundamental principles of molecules and structures with at least one dimension between 1 to 100 nm, while nanotechnology is the application of these structures into useful nanoscale devices[1].The impact on society and our lives of the continuous downscaling of microelectronic systems is profound, and continues to open up novel frontiers and possibilities. The excitement generated by nanoscience and technology is a result of these efforts and our desire to explore arenas which have till now been left unexplored. The physical properties of solid materials at the nanoscale are much different as compared to their bulk properties. These include lowering of melting point, single electron charging, novel magnetic and optical properties etc.[2] The oldest example of an application of these properties are the stained glass windows found in medieval and Victorian churches and glazes found on ancient potteries. The beautiful colour they exhibit is due to the presence of nanoscale metal particles, which show a wide range of colours depending on their shape and size. In 1959, in a now famous speech, given to the American Physical Society, Richard Feynman discussed how to manipulate and control matter on a molecular scale in order to achieve electronic and mechanical systems with atomic sized components[3]**.** In recent times, with the advancement in technology, new tools for characterization like scanning probe microscopes were discovered. This has provided an impetus to research in this area as it was possible to observe and characterize the processes at the nanoscale.

There are two possible approaches of nanofabrication, namely the "top-down" approach and the "bottom-up" approach. In the top-down methods, the features are written directly onto a substrate, for example, by an electron beam, and then transferred to the underlying substrate by applying appropriate etching and deposition processes. In the bottom-up approach, nanocomponents are first synthesized from precursors in liquid, solid or gas phase and then employing either chemical or physical processes. Then they

are used as building blocks and integrated to form the final device structure. The top-down approach has an advantage of being compatible with the current microelectronic processing methods. However, as we decrease the feature size, the cost involved increases exponentially and also as the feature size approaches the wavelength of the light source, imperfections are observed at the interfaces due to diffraction effects. Bottom-up approach on the other hand involves arranging nanoscale building blocks in a desired fashion to give the final device structure. Bottom-up approach is comparatively cheaper since it doesn't require high capital cost. A variety of nanoscale building-blocks (e.g. nanoparticles, nanotubes, nanowires, etc.) exist and the list continues to grow with breakthroughs in synthesis techniques. For bottom-up approaches, self-assembly is generally regarded as the most promising technique for designing and controlling the assembly of nanometer-scale objects into structures such as sheets, tubes, wires, nanoelectronic devices and drug delivery systems[4]. The application of nanotechnology to areas such as photonics and electronics, chemical and biological sensors, energy storage, and catalysis requires the manipulation of these nano-objects into functional materials and devices that are addressable at the nanoscale. Hence a control over ordering and patterning of nanobuilding blocks is an essential requirement.

1.2 Project Description:

The pursuit of converting the existing scientific knowledge and understanding into functional end products is the ultimate aim of any research. As discussed earlier, there has been a lot of research in the field of nanotechnology in the last few decades owing to the advances in characterization techniques. A greater depth of knowledge has been created and the next step of converting this into useful devices is in progress. The present work tries to take a step further in a similar direction. Our objective is to fabricate gold nanoparticle arrays for subsequent device fabrication. Nanowires are important building blocks for next generation nanoelectronics as well as for varied applications like solar cells, sensors, catalysts etc. One of the most convenient method to synthesize a variety of nanowires is through VLS process utilizing gold as the catalyst.[5,6] A number of such recipes have been reported in the literature[7] but control over ordering and density of wires is yet to be achieved. In the VLS process, nanowires are grown with gold as seed in

a CVD furnace in the presence of a precursor gas. Since gold particles act as seeds, the ordering and the density of the nanowires is governed by the initial arrangement of gold dots on the surface. Hence a control over the arrays of dots will ultimately transform into the ordering of nanowires. Currently, nanoparticles are arranged on the substrate using methods like Laser Ablation[5], thin film deposition[8] or by electrophoretic deposition[7]. All these methods have limited control over the arrangement of catalyst on the substrate and hence on the nanowire size and density.

The current project aims at fabricating ordered MPN arrays and removing the surfactant covering of the particles without disturbing their lateral arrangement. The three basic steps involved are:

1. Synthesis of Gold Nanoparticles
2. Fabrication of MPN arrays
3. Removal of the protective ligand without disturbing the order

This report has three chapters tat discuss the progress made in implementing these three basic steps and ends with a chapter on conclusion.

References

[1] Ratner, M., & Ratner, D., '*Nanotechnology, A Gentle Introduction to the Next big Idea*', Pearson Publications(2005).

[2] Marcell and Dekker, *'Encyclopedia of Nanoscience and Nanotechnology'*, 1829-1840 (2004).

[3] Feymann, R., '*There's Plenty of Room at the Bottom',* at the annual meeting of the American Physical Society at the California Institute of Technology (Caltech), December 29th 1959.

[4] Whitesides, G.M., & Grzybowski, B., *'Self Assembly at all scales'*, Science **295,** 2418-2421 (2002).

[5] Morales, A.M.; Lieber, C.M.; *'A Laser Ablation method for synthesis of crystalline Semiconductor Nanowires'*, Science, 279,208-211(1998).

[6] Wu, Y.; Yang, P., *'Direct Observation of Vapor-Liquid-Solid Nanowire Growth'* J. Am. Chem. Soc.; (Communication); **123(13)**; 3165-3166(2001).

[7] Hochbaum, A.I.; Fan, R.;Rongui He;Yang P.; *'Controlled Growth of Si Nanowire Arrays for Device Integration'*, Nano Letters, **5(3),**457-460(2005)

[8] Saif, I.; Sharma, S;Kamins, T.I.;Stanley,W.R.; *'Ultrahigh-density silicon nanobridges formed between two vertical silicon surfaces'*, Nanotechnology, **15(5)**, L5-L8(2004)

Chapter 2: Synthesis of Nanoparticles

2.1 Introduction

The first step towards the fabrication of nanoparticle arrays is to synthesize the building blocks i.e. monodisperse nanoparticles. Monodisperse nanoparticles are necessary since polydispersity will lead to disorder in the patterns formed, rendering it unfit for electronic and other applications that require addressing at the nanoscale.[1] Various methods have been reported in literature for the synthesis of different types of nanoparticles[2,3]. Synthesis can be achieved either in gas or liquid phase. Gas phase synthesis involves evaporation of metal atoms and subsequent condensation in an inert gas atmosphere. Mean particle size is controlled by oven condition and flow rate of inert gas.[2] Gas phase synthesis has the advantage of providing good control over size of the particles, but involves high capital and operating costs as compared to the solution phase synthesis techniques. Solution phase syntheses involve reduction of precursor metal salts using chemicals in liquid phase. A comprehensive review of several solution phase synthesis strategies is given by Cushing et al.[2] Synthesis routes reported by Brust et al[3] and Giersig et al[4] are two commonly used liquid phase techniques for making gold nanoparticles of smaller(<5nm) and larger(>5nm) sizes respectively. Wu et al[5] and Wang et al[6] have reported attractive alternative synthesis routes that promise good control over shape and size of the nanoparticles. Turkevich et al[7] report gold nanoparticles of size around 20nm using sodium citrate as the reducing agent to reduce $HAuCl_4$. Mulphrodt[8] modified Turkevich[7] method by using tannic acid as an additional reducing agent. Slot and Geuze[9] modified the scheme further and reported synthesis of Au nanoparticles ranging from 3 to 17nm in size by varying the concentration of tannic acid(TA).

The nanoparticles formed have an inherent tendency to agglomerate and form larger aggregates, so as to minimize their surface energy. To avoid agglomeration, these particles need to be stabilized either by electrostatic stabilization or by steric stabilization. In the former, a layer of ions adsorbed on the surface prevents the nanoparticles from coming in close proximity, while in the latter case, long molecule chains attached to the surface of the particles serve the purpose. The stabilization could be changed from one

form to the other (called change in surface functionality) and is generally dictated by the application where these molecularly protected nanoparticles (MPNs) have to be utilized.

2.2 Characterization Details

UV-Visible Spectrophotometer (Shimadzu 2401) was used to characterize MPNs in solution phase. The intensity of light (wavelength range 200nm to 900nm) passing through a sample (I), kept in a quartz cuvette (Plastibrand, 1 cm path length) is measured and compared with the intensity of light before it passes through the sample (I_o). The absorbance, A, is calculated as $A = -\log (I_o/I)$, and plotted as a function of wavelength.

At nanometer dimensions, the free electron cloud in a metallic nanoparticle oscillates on the particle surface and absorbs electromagnetic radiation at a particular resonant energy.[10] This resonance, known as plasmon resonance, is a property characteristic of nanoparticles. Different nanoparticles give plasmon peak at different wavelengths. Also the peak position shifts according to the shape and size of the particles as well as their physical environment like solvent and capping.[10,11] For 10nm sized particles, colloidal gold displays plasmon resonance around 530nm while silver does so at 350nm wavelength.[12] This phenomenon is utilized in UV-Vis spectroscopy to indicate the presence of nanoparticles.

Size of nanoparticles can be estimated using Dynamic Light Scattering (DLS), which utilizes the property of Brownian motion of the particle to calculate its diameter. Brookhaven DLS instrument (Model BI-200SM) was used to obtain the size distribution and polydispersity of the particles. The diameter obtained from DLS is the hydrodynamic diameter based on the diffusion coefficient of the particle. It is normally more than the actual diameter. The data obtained from the DLS is in the form of a distribution of particle sizes based on their relative intensities. To calculate the particle size distribution, a Gaussian curve is fitted to the dominant mode of the intensity distribution using Origin software and mean (μ) and linewidth (Γ) calculated. Standard deviation (σ) is calculated using the relation [$\sigma = 0.849*\Gamma/2$][13] while percentage polydispersity is obtained as $\sigma*100/\mu$. For multimodal distribution the method of non negative least square(NNLS) was used while in the case of unimodal distributions, the polydispersity is taken as the

square root of the value reported by Cumulants algorithm. In the intial experiments, only one run was conducted to get the data. Later, based on ISO standard(13321), six runs for each sample were conducted and mean of the peaks and polydispersity are reported with standard deviation.

2.3 Results and discussion

Three different synthesis schemes were tried in pursuit of getting stable and less polydisperse nanoparticles. These are discussed in detail in subsequent sections. As stated previously our objective is to synthesize Au nanoparticles with a good control over size and reproducibility. Since we were interested in particle sizes in the range 5 to 10 nm, we chose the synthesis methods described by Wu et al[5], Wang et al[6] and Slot et al[9]. As reported these methods provide a good control over shape, size and polydispersity of the nanoparticles formed. The information regarding chemicals used in all the experiments alongwith the purity and supplier is provided in Appendix-V. All chemicals were used as obtained without further purification. The water used was deionized water obtained from Millipore instrument with a specific resistance of 18.2 MΩ-cm. Glass wares were rinsed with aqua regia to remove any traces of impurities and then washed with a lot of tap water. Finally they were rinsed in distilled water and ethanol and dried in a laminar hood before use.

2.3.1 Sonomechanical method

Wu et al.[5] reported the preparation of metallic nanoparticles by sonomechanical-assisted metal displacement reaction. Spontaneous electrochemical reaction occurs when a metal foil is inserted in a solution containing dissimilar metal ions. The metal ions in the solution get reduced to zerovalent atom state while the more electropositive metal foil gets oxidized. The particles formed on the surface are dislodged due to the pressure waves generated by sonication.

For the synthesis of Au nanoparticles, Aluminium foil (98% purity) was cleaned using chromic acid and boric acid to remove any alumina layer on it[14]. 2.5mM $HAuCl_4$ (Kemie labs) solution in deionized water was mixed with 50mM PVP(polyvinyl pyrrolidone) solution in equal volumes of 5ml each and sonicated after inserting the

Aluminium foil. The colour of the solution changed from light yellow to dark blue after 7 minutes. UV Visible absorption spectra of the sample was recorded before and after sonication with 50mM PVP solution as reference(Fig. 1).

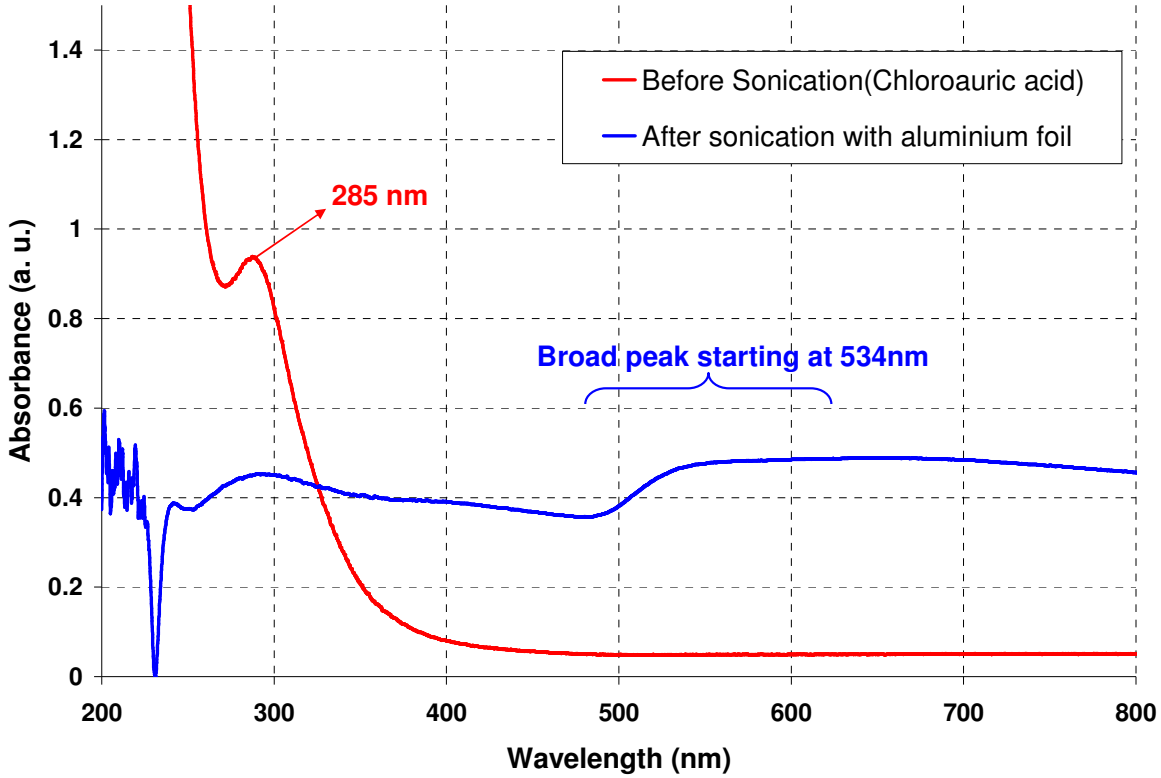

Figure 1: UV-Visible Absorption spectra of solution initially containing Gold chloride before and after sonication with Aluminium foil

The reported peaks in the spectra for $HAuCl_4$ solution in water is around 280nm, while for PVP stabilized gold colloidal particles it is around 530nm[15,5]. As seen from fig 1, before sonication there is a distinct peak at a wavelength of 285 nm indicating the presence of $HAuCl_4$ in the solution. After sonication, there is a broad peak at a wavelength of 530nm alongwith a peak at 295nm indicating the presence of nanoparticles and unreacted $HAuCl_4$. The breadth of the peak starting at 520nm implies that particles with various shapes and sizes are present in the solution. The mixture was centrifuged after adding equal volume of 1mMol dodecanethiol in ethanol and the resultant solution was analysed through DLS. The results indicated the presence of particles of average size 347nm. The DLS of PVP solution did not indicate any particles of this size range.

Since, we were unable to reproduce the reported results, this method was not pursued further.

2.3.2 Liquid Solid Solution (LSS) method:

Wang et al.[6] report a unified approach for the synthesis of a large variety of monodisperse nanocrystals with different chemistries and properties. The method involves three phases, liquid-solid-solution (LSS). In case of synthesis of Au nanoparticles these three phases are: $HAuCl_4$ in water and ethanol (liquid), sodium salt of fatty acid(solid) and mixture of ethanol and fatty acid(solution). Mixture is kept in an autoclave tube and heated at specific temperature depending on the size of the nanoparticles desired. The main reaction is reported to be the reduction of noble metal ions by ethanol at solid-liquid and solid-solution interface. In case sodium linoleate is used, initially a phase transfer process at the water-ethanol solution and the sodium linoleate interface is reported to lead to the formation of Au-linoleate, which is subsequently reduced by ethanol to Au^o. The fatty acid formed *in situ* caps the nanoparticles and creates a hydrophobic surface around them. Due to their incompatibility with the hydrophilic surroundings, these particles precipitate and are collected at the bottom of the vessel. Concentrations and temperature are the main controlling parameters of the LSS strategy. As reported, to get nearly monodisperse nanocrystals, optimal concentration conditions are usually kept in the range of 0.03-0.12 mol/l. Park et al[16] have also reported a similar strategy for making Fe_2O_3 nanoparticle. They first synthesize the metal-oleate complex and then heat it in a high boiling point solvent. In the case of noble metal salts, isolation of metal-oleate complex is not facile due to its low stability at room temperature.

Experiments were carried out using oleic acid, sodium oleate and aqueous $HAuCl_4$ solution due to non-availability of the linoleic acid-salt pair. According to Wang et al[6] the temperature for the reaction decides the size of the nanoparticles. Gold nanoparticles of 6nm size were synthesized at a temperature of 60^oC, while smaller particles were reportedly synthesized at lower temperatures using linoleic acid-salt pair. Also, they claim that the use of stearic acid-salt pair gives monodisperse particles for gold, only at a

temperature of 180^{o}C. Stearic, Oleic and Linoleic acids are both C_{18} acids and differ only in the number of double bond they contain. Linoleic acid contains two, while oleic and stearic acid contain one and zero double bonds respectively. Based on this alongwith the fact that their melting points are -5^{o}C(Linoleic acid) and 15^{o}C(Oleic acid), it was decided to choose the temperature in the range of 60-80^{o}C for synthesizing 6nm size particles. The concentration of gold sol was taken as 0.1 mol/l and the whole reaction was scaled down by a factor of two as compared to the reported values. Quantity of oleic acid, ethanol and sodium oleate was taken as reported in the paper after scaling them down appropriately.

Reaction was carried out in a Parr reactor(Parr Instrument co, USA, Model 4744) and reaction mixture was kept in an oven at the specified temperature for 10 hrs. At the end of the reaction, two distinct phases were visible. The top layer mostly comprising of the oleic acid, while the bottom layer containing some black residue and water. The top layer was discarded and the black precipitate in the bottom layer was carefully separated and dispersed in different organic solvents like chloroform, cyclohexane. It was observed that for all solvents, the colour of the solution obtained was bluish and the solutions were not stable with time. Presence of oleate was speculated to be the probable reason for this instability. Hence, in the next few experiments, first the bottom layer was washed with ethanol to dissolve and remove any oleate present, centrifuged and then re-dispersed in cyclohexane or chloroform. Still the blue colour persisted and the solution was not stable. UV-Vis analysis also didn't show any surface plasmon peak for gold nanoparticles instead it showed a very broad and weak peak indicating the presence of various shapes and sizes of nanoparticle. (Fig. 2)

During the experiments, it was also observed that the top layer always showed wine red colour. To investigate this, UV-Vis of the top layer was measured with oleic acid as the background, since the top layer mostly contains oleic acid.(Fig. 2) The results showed a peak around 525 nm confirming the presence of gold nanoparticles in the top layer.

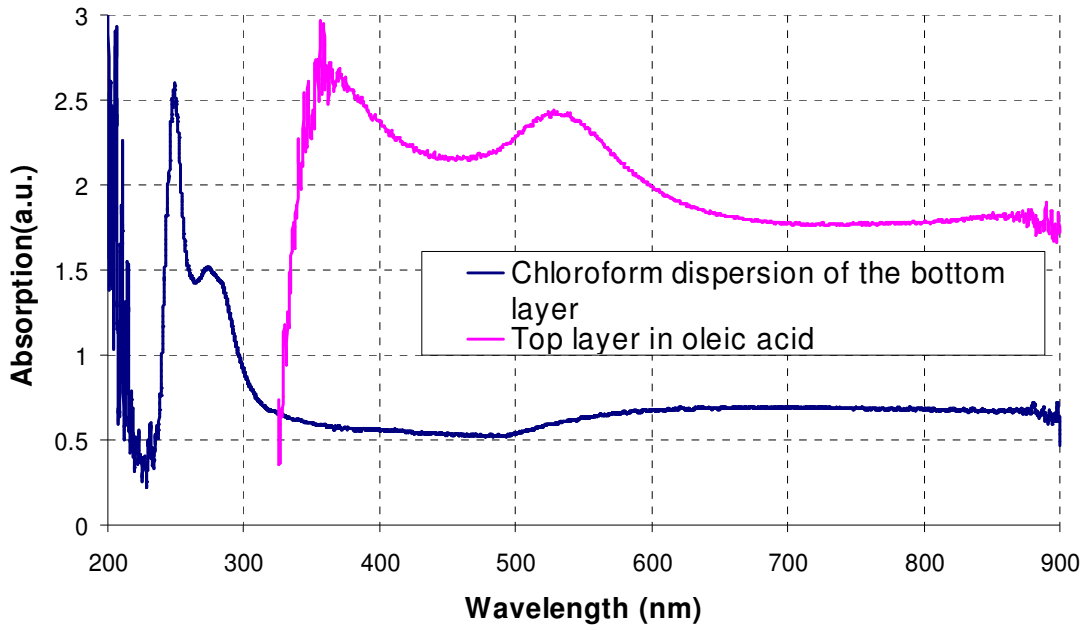

Figure 2: UV-Visible Absorption spectra of chloroform dispersion of the bottom layer and Oleic acid solution of the top layer obtained in LSS experiment

Based on this observation, in the next few experiments, we attempted to isolate the particles from the top layer of the final product. Also to observe the temperature effect on the size of the particles, the experiments were conducted at different temperatures. The UV-Vis spectrum of the top layer for experiments conducted at 24^{o}C and 60^{o}C with oleic acid as the background is shown in fig. 3. Wang et al[6] report that an increase in temperature causes an increase in the size of the particles. Also the surface plasmon resonance of the gold nanoparticles shows a red shift with increasing particle size. As observed in the figure 3, the peak for the experiment at higher temperature is at 539nm, while for lower temperature it is at 525nm indicating the presence of smaller size particles for lower temperature[10], in accord with the reported data. The DLS data for reaction at 24^{o}C revealed particles of size 17 nm with a polydispersity of 3% while for the 60^{o}C experiment, the sample was too dirty and could not be analysed by DLS.

After confirming the presence of nanoparticles, the next step was to isolate these particles in some organic medium so that we can cast them over water surface to form monolayers of nanoparticles. Immediate discoloration of the layer was observed on

addition of organic solvents to an aliquot of top layer. The only solvent in which it was found to be stable was oleic acid. This is in contrast to the reported results which says that the bottom product can be easily dispersed in any organic solvent and is stable.[6] The reason maybe attributed to the weak capping of the nanoparticles, which got dislodged as soon as the medium is changed.

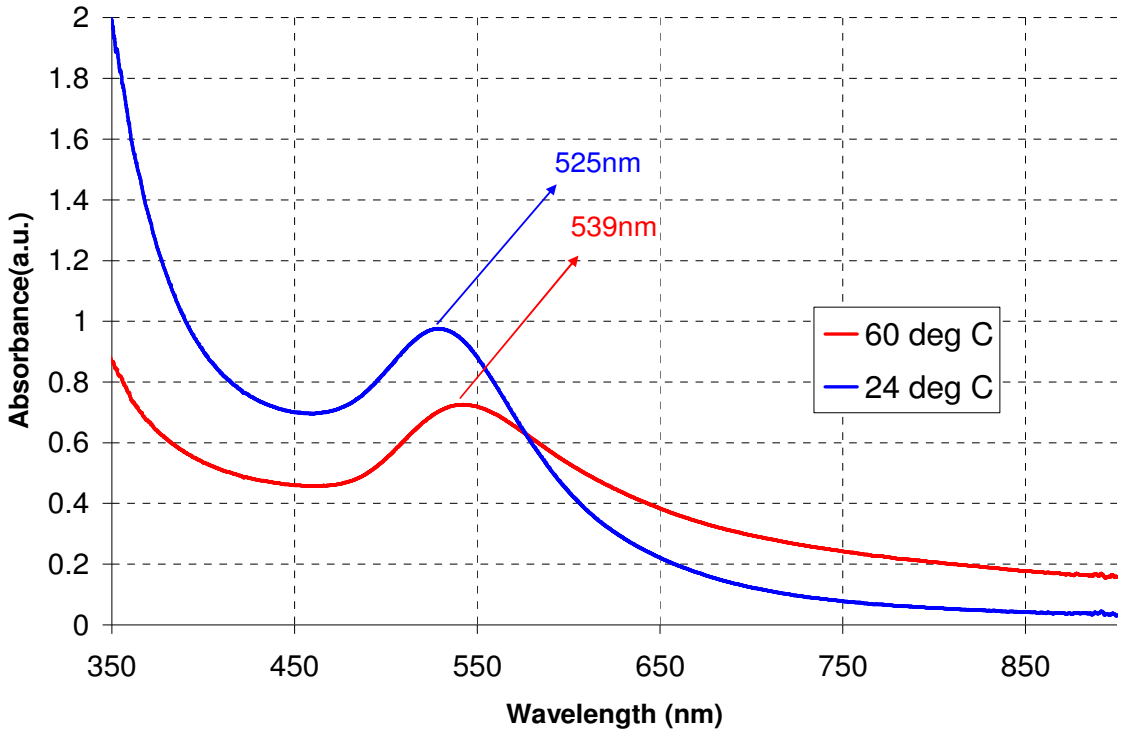

Figure 3: UV-Visible Absorption spectra of oleic acid solution of top layer of LSS experiment for different temperature conditions

To observe if we can directly disperse the particles in n-hexane *in situ* during the reaction, some amount of n-hexane was added to the top layer before starting the experiment. At the completion of the reaction the whole top organic layer showed wine red colour but when we tried to evaporate n-hexane in air over water surface to get a self assembled monolayer, it was observed that the residue formed tiny oily drops, which were pink in colour. The explanation for this lies in the fact that although n-hexane has a low boiling point (69^{o}C), the sample also contains oleic acid dissolved in it, which has a very high boiling point (360^{o}C). So, when we try to evaporate the top layer, n-hexane

evaporates but the oleic acid remains and the nanoparticle having a hydrophobic end, prefer to stay in the islands formed by oleic acid.

Although there are various phase transfer protocols available in literature[21], yet none of them reports transfer of carboxylic acid stabilized nanoparticles from carboxylic phase to aqueous phase. Also it seemed to be a cumbersome process to transfer the particles from organic(oleic acid) phase to aqueous and then back to another organic having lower boiling point like n-hexane, critical for our objective of making arrays. Based on all the above experiments it was deduced that it may not be possible to isolate particles from this method for making NP arrays.

2.3.3 Tannic acid Method:

Muhlpfordt[8] first described a method of making nanoparticles using a combination of tannic acid and trisodium citrate as reducing agent. This is an extension of the Turkevich[7] method, which gives 20nm size gold nanoparticles using only sodium citrate. The method, later extensively studied and described in detail by Slot et al[9], has been used by various researchers to produce gold nanoparticles ranging from 3 to 17 nm in size. Control over size is achieved simply by changing the concentration of tannic acid. (See table. 1).

1% Tannic acid amount (for 100ml final solution)	**Gold Particle size[17]**
5.00	3.5
2.50	4.0
1.00	5.0
0.50	6.0
0.25	7.5

Table 1: Particle size distribution with different TA concentration

The experimental protocol as reported to make 100 ml of gold sol is as follows. Two solutions (a) and (b) are prepared initially:

(a) 1ml of 1% (w/v) hydrogen tetrachloroaurate(III) trihydrate($HAuCl_4.3H_2O$) solution, added to 79 ml of deionized(DI) water,

(b) The reducing mixture consists of 4ml of 1% (w/v) trisodium citrate dihydrate ($C_6H_5O_7Na_3.2H_2O$), selected volumes (0.01–5 ml) of 1% tannic acid ($C_{76}H_{52}O_{46}$), and DI water to produce a final volume of 20 ml. In case the amount of Tannic Acid (TA) used was more than 1 ml, an equivalent amount of 25mmol K_2CO_3 was added to maintain the pH in the range of 7.5 to 8.0.

Both (a) and (b) solutions are heated to 60±1^oC on a hot plate and then the reducing solution (b) is rapidly added while vigorously stirring the hydrogen tetrachloroaurate (III) tetrahydrate solution. Stirring must be carried out until the end of the reaction. After the color of the mixed solution turns to red, the solution is heated to boiling for about 10 min and finally the solution is cooled with chilled water.

As reported by Slot et al[9], the average particle diameter went down from ~17 nm when 10 µl of 1% TA was used to values approaching 3 nm when it was increased to 5ml. The temperature (60^oC) was chosen as a trade-off between the size and polydispersity of the particles. Higher temperature resulted in polydisperse nanoparticles while lower temperatures caused increase in the particle size. Also for making smaller size particles, it is reported that pH should be in the range of 7.5 to 8. Higher pH values resulted in polydispersity, while lower pH caused formation of larger particles. Rate of stirring and the size of beakers should be chosen so as to provide rapid mixing.

The reason, as explained by Slot et al,[9] for the control over the size of particles is due to the difference in the reducing capacity of tannic acid and citrate. Tannic acid causes a fast reduction, while citrate reacts slowly. Therefore, when excess of tannic acid is used, reduction is mostly done by TA only, while when lower quantity is used, tannic acid gets exhausted and citrate takes over to complete the reduction process. In case when no TA is used, 20 nm size particles are formed.

Initial experiments were conducted by scaling down the experiment to a total volume of 50 ml and with tannic acid volumes ranging from 1.5 to 3ml, which correspond to 3 to 6ml in the actual synthesis scheme.[9] This range was chosen based on the data reported to get particles of the range 4-5nm. The UV-Vis plots are shown in fig. 5. The “blank” in the figure denotes the experiment without any $HAuCl_4$ with rest of the conditions same and TA volume corresponding to 1.0 ml. Interestingly, though all the final solutions except the “blank”, obtained were wine red in colour, the UV vis peak was not as

predominant and was observed only as a slight kink at values around 515-525nm. The reason may be that all the UV-Vis spectra were measured with water as background, TA present in the solution causes interference with the surface plasmon resonance of gold nanoparticles. The resulting UV-Vis spectra look similar to those reported by Wong et al[16] for same concentration and synthesis route.

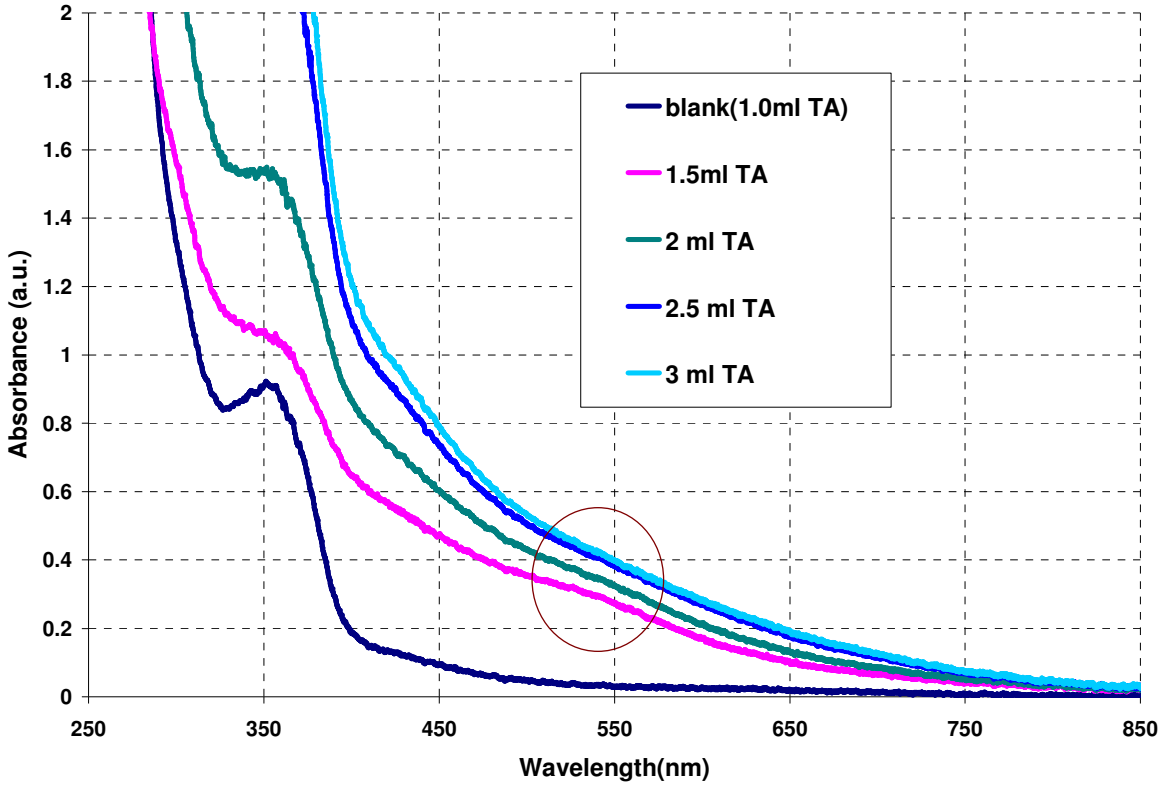

Figure 4: UV-Visible Absorption spectra of gold sols prepared via tannic acid route for different TA concentrations

Further experiments were conducted with 0.5ml, 0.75ml, 1 ml and 3ml TA with 100ml total volume of the mixture. The experiments were repeated to ensure reproducibility. The particle size was measured using DLS.(Table 2) As reported by Slot et al[9], it is observed that the size of the particle decreases with increasing TA concentration although not much difference was observed between 0.5, 0.75 and 1ml TA concentration. Also the size of the nanoparticles obtained in the experiments are larger as compared to what is reported by Slot et al.[9] This may be attributed to the difference in the mixing rates and the source of the tannic acid used for the experiments. Also the size characterization was done using DLS in our

experiments while the data reported by Slot et al is obtained by TEM images.[9] It is also seen that when the volume of the reaction solution is changed, the size of the nanoparticles synthesized are affected.

S. No.	Experiment Conditions (total volume in bracket)	Size by DLS(nm)		Size reported by Slot et al[9] (nm)
		Mean	Polydispersity %	
1	0.5 ml TA(100ml)	10.4	10.2	6.0nm
2	0.75 ml TA(100ml)	9.6	7.1	5.5nm
3	0.75 ml TA(100ml)	8.8	4.3	
4	1.0 ml TA (100 ml)	10.4	6.1	5.0nm
5	1.0 ml TA (100ml)	10.2	6.2	
6	3ml TA (50ml)	5.0	11.0	4.0nm
7	3ml TA (100ml)	6.2	7.5	
8	Blank(no $HAuCl_4$ but same experimental protocol with 3ml TA)	174.1	7.0	

Table 2: DLS size data for gold sols prepared via tannic acid synthesis route

Note: Data based on single run for each sample

Another observation was that the DLS results always indicated presence of peak around 150nm to 200nm range. It was speculated to be because of the TA present in the solution. In order to clarify this, a blank experiment was conducted containing 3ml TA but without adding any gold salt. Other experimental conditions were kept constant. DLS results of samples from this experiment indicate the presence of particles of size around 174 nm. (Table. 2) Also, it was observed that the colour of the solution of blank experiment changed from pale yellow to brownish green with time. This was probably due to the polymerization of tannic acid.[9,19] UV-Vis spectrum of a blank experiment(fig. 6) with 3 ml TA was done and its variation with time observed. The results show changes in the peaks implying that the structure of tannic acid is evolving with time.

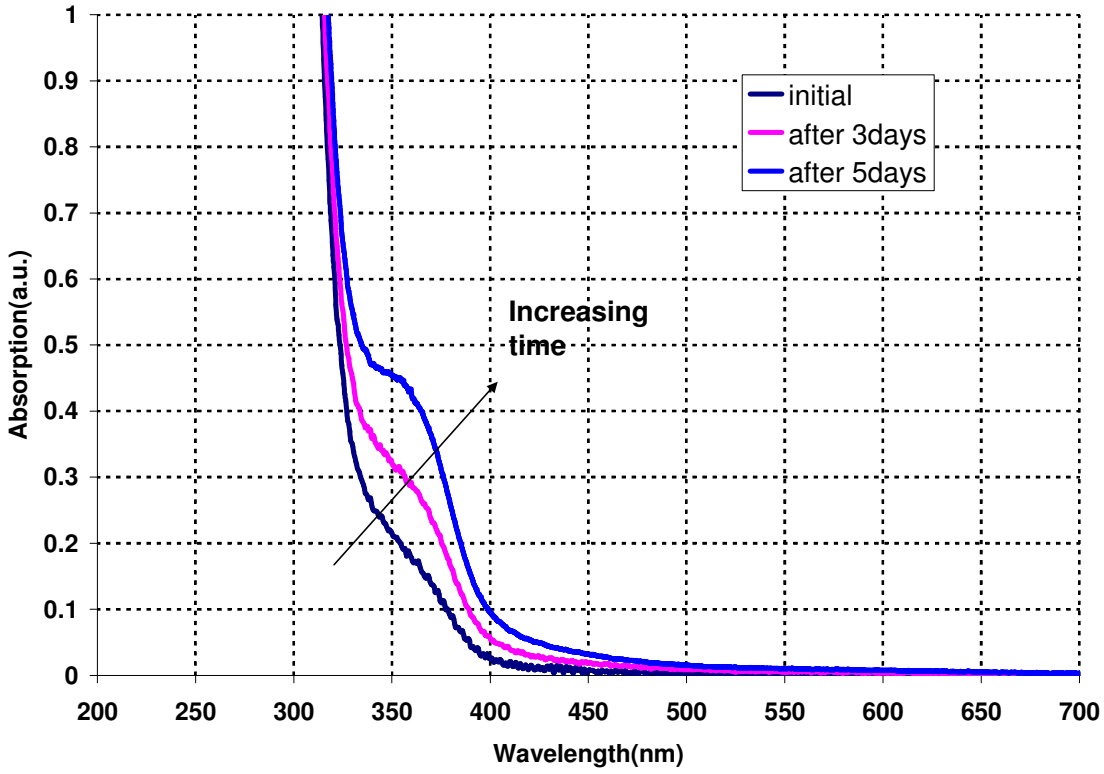

Figure 5: Variation of UV-Vis spectra with time for experiment conducted without any gold salt

Simultaneously, capping and redispersing the nanoparticles in organic solvent was also tried. We chose n-hexane as the solvent and dodecanethiol as the capping agent. This is because the low boiling point of n-hexane is suitable for array formation and high affinity of –SH group with the gold provides a very stable capping of the nanoparticles. The experimental protocol followed was as given by Huang et al.[20] Briefly, around 1 ml of gold colloid was added dropwise to 1ml of 1mmol dodecanethiol solution in ethanol, with intermittent stirring. The sample was kept for 24 hrs and then centrifuged at 3500 rpm for 1 hour. The supernatant was removed carefully and precipitate was allowed to dry overnight. This precipitate was then redispersed in n-hexane using sonication. The UV vis spectra of the sample (5ml TA) before and after the sonication are shown in fig. 7.

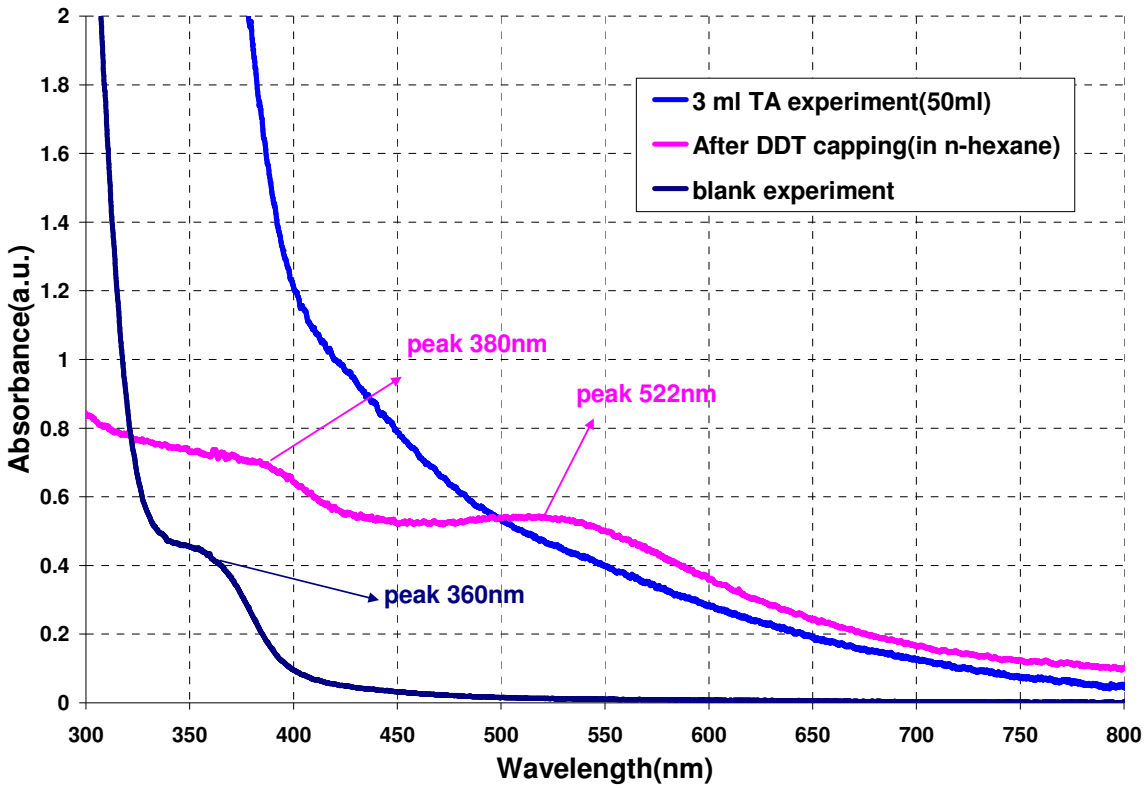

Figure 6: UV-Vis Absorption spectra of gold sols prepared via TA route before and after capping dodecanthiol

As observed in the figure, the peak corresponding to tannic acid was still present. This implies that TA was not removed completely during the capping process. If allowed to remain in solution, it will polymerize and will cause problems later while we are trying to fabricate arrays. Conductivity measurements also indicated difference in the conductivity of standard gold sol(commercial) vis-a-vis the gold sol produced by us.(Table 3) The reason for difference may be due to the presence of tannic acid ions in the solution.

S. No.	Experiment details	Conductivity(μS/cm)
1	3ml TA blank	868
2	0.75 ml TA blank	533
3	0.5 ml TA blank	537
4	3ml TA gold sol	823
5	0.75ml TA gold sol	615
6	0.5ml TA gold sol	580
7	Commercial gold sol	**412**

Table 3: Conductivity data for various concentrations of TA and gold sols

Giersig and Mulvaney[4] have reported an ion exchange method, using Amberlite MB-1, for the removal of Tannate ions and citrate ions that decreases the solution conductivity to a value of 2 µS/cm. Liou et al[19] have reported boiling with H_2O_2 to neutralize excess tannic acid present in the solution. To remove TA, in the next experiment, gold sol prepared using 0.75 ml TA was taken and H_2O_2 was added, such that the overall concentration of H_2O_2 in the solution was 0.2% and the solution was boiled for five minutes. The UV-Vis spectra of solution before and after the treatment is shown in fig 8. As observed from the curves, after boiling with H_2O_2, the peak observed due to TA vanished and subsequent capping also did not indicate any peak in the 350-400 nm region indicating removal of TA. The DLS analysis(fig.9(a),(b)) shows two peaks for the sample before boiling, one near 9.6±1.6 nm while other around 158.3±24.3 nm. After boiling the DLS data shows a peak at 8.8±0.9 nm while the peak around 160 nm has vanished and instead we have a peak at 50.3±5.1 nm. The reason for the 50 nm peak may be attributed to insufficient neutralization of tannic acid. This indicates removal of TA from the solution to a certain extent.

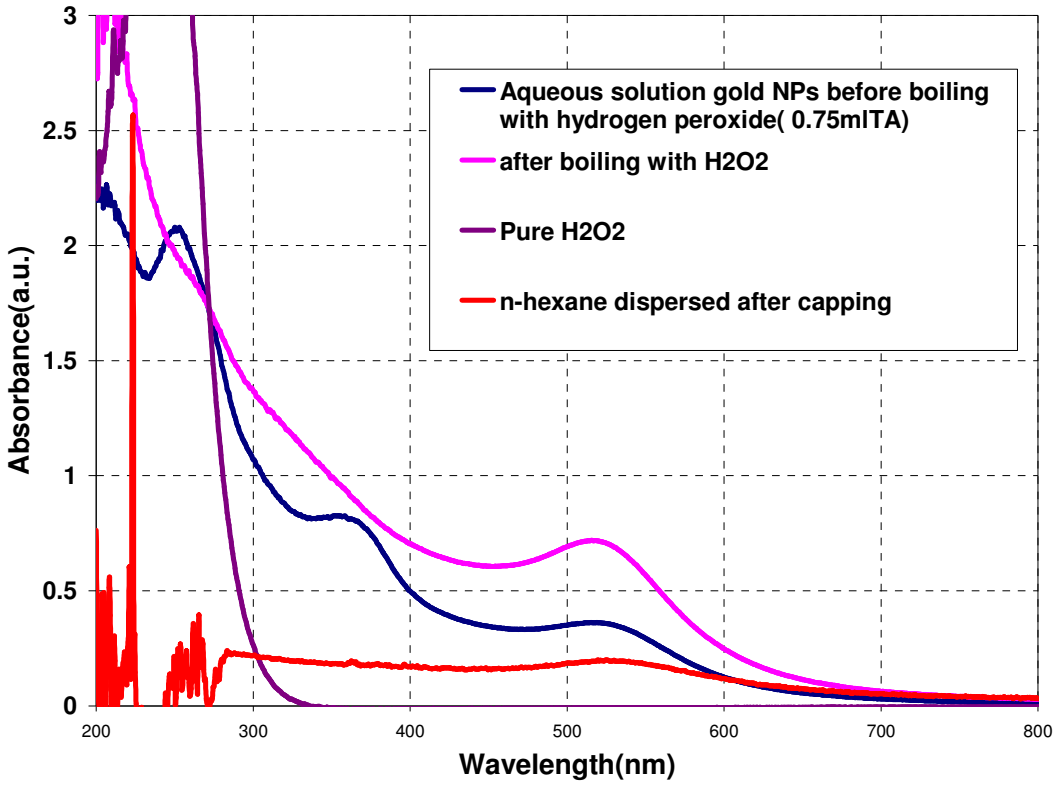

Figure 7: UV-Visible absorption spectra of solution after boiling with hydrogen peroxide

This suggested that a proper tuning of the experiment was required. To analyse the affect of H_2O_2 a series of experiments was conducted, slowly increasing the peroxide concentration. The UV-Vis spectra of the same are shown in fig. 9. It can be seen from the data that the peak for tannic acid decreases with increasing peroxide concentration. The DLS data also confirmed this, by the absence of particles of size 154 nm.

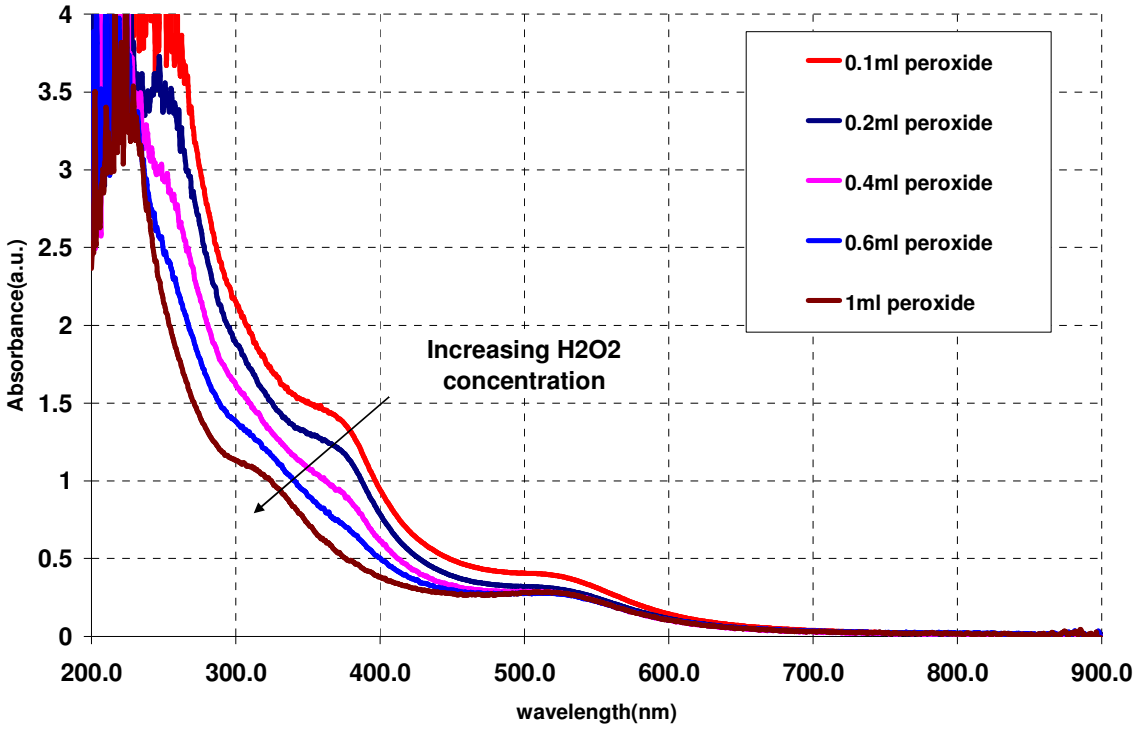

Figure 8: Effect of boiling with different peroxide concentration

Further tuning of parameters like amount of K_2CO_3 and time of boiling were optimized and a standard protocol for synthesizing particles with size ranges around 5nm and 10nm was developed and verified for reproducibility. The standardized experimental protocol is given in Appendix-I. The DLS analysis and the experimental details for both size ranges are given in Table 4. It is to be noted that the peaks obtained from the DLS gives the hydrodynamic diameter of the particle which are larger than the true diameter.

S.No.	Size range	Experiment details	DLS results		Remarks
			Peak	Polydispersity	
1.	5nm	3ml TA, 1.0ml H_2O_2	7.1±0.90	12.7±3.45%	*Data based*
2.	10nm	0.1ml TA, 0.1ml H_2O_2	12.7±0.62	10.0±2.96%	*on six runs*

Table 4: DLS data for particles of nominally 5 nm and 10 nm size in aqueous phase

2.4 Conclusions:

Our aim was to synthesize gold nanoparticles with a control over the size, and polydispersity. The sonomechanical method and the LSS method were not able to provide us with a feasible solution due to reasons explained above. Tannic acid synthesis route gave better control over particle size distribution as well as reproducibility. A protocol for synthesizing gold nanoparticles of two different size ranges free from impurities has been developed and could be used for further experiments. In the next chapter we will discuss about the capping of these nanoparticles and fabrication of arrays.

References

[1] Whitesides, G.M.; Grzybowski, B.; *'Self Assembly at all scales*', Science **295,** 2418-2421 (2002).

[2] Cushing, B.L.; Kolesnichenko, V.L.; O'Connor, C.J.; *'Recent Advances in the Liquid-Phase Syntheses of Inorganic Nanoparticles*', Chem. Rev.,**104,**3893-3946 (2004).

[3] Brust, M.; Walker, M.; Bethell, D.; Snhiffrin D.J.; Whyman, R.; *'Synthesis of thiol-derivatised gold nanoparticles in a two-phase liquid-liquid system',* J.Chem.Soc.*,* **Chem. Commun.,** 801-802 (1994).

[4] Giersig M; Mulvaney, P., *'Preparation of ordered monolayers by electrophoretic deposition*', Langmuir **, 9(12),** 3408 (1993).

[5] Wu, C.,;Mosher, B.P.; Zeng, T.; *'Rapid synthesis of gold and platinum nanoparticles using metal displacement reduction with sonomechanical assistance*', Chem. Mater., (Commun.), **18(13),** 2925-2928 (2006).

[6] Wang,X.; Jing Z.; Qing, P.;Yadong. L.; *'A general strategy for the nanocrystal synthesis'*, Nature (Letters to Editor), **437,** 121-124 (2005).

[7] Turkevich, J.; Stevenson, P.C.; Hillier, J.; *'A study of the nucleation and growth processes in the synthesis of colloidal gold*', Discuss. Faraday Soc., **11,** 55-75(1951).

[8] Muhlpfordt, H., *'The preparation of colloidal gold particles using tannic acid as an additional reducing agent'*. Experientia ,**38**, 1127-1128(1982).

[9] Slot, J.W.;Geuze, H.J., *'A new method of preparing gold probes for multiple-labeling cytochemistry*', European Journal of Cell Biology, **38,**87-93(1985).

[10] S. Link; M. A. El-sayed; *'Spectral properties and relaxation dynamics of surface plasmon electronic oscillations in gold and silver nanodots and nanorods'*, J. Phys. Chem. B, **103,** 8410-8426(1999).

[11] C. Noguez, *'Surface Plasmon on Metal Nanoparticles: The Influence of shape and Physical Environment'*, J. Phys. Chem.C, **111(10),** 3806 -3819(2007).

[12] Christophe, P.;Patricia, L.; Pileni, M.P.; '*In situ synthesis of nanocluster in AOT reverse micelles'*, J.Phys.Chem.,**97**(12974-12983).

[13] http://hyperphysics.phy-astr.gsu.edu/hbase/math/gaufcn2.html#c1 *accessed on 20.10.06*

[14] http://www.faradnet.com/ *accessed on 30.06.06*

[15] Daliparthi, S.P.R., *'Synthesis and characterization of gold nanoparticles*', **ME thesis**, Indian Institute of Science (2006).

[16] Park, J., *'Ultra Large scale syntheses of monodisperse nanocrystals*', Nature Materials, **3,**891-895(2004).

[17] http://www.hei.org/research/aemi/gold.htm#TAconc. *Accessed on 10.11.2006*

[18] Michael O.Nutt; Heck, K.N.; Alvarez, P.; Wong, M.S., *'Improved Pd-on-Au bimetallic nanoparticle catalysts for aqueouos-phase trichloroethene hydrodechlorination'*, Applied Catalysis B:Environmental, **69(1-2)**,115-125(2006).

[19] Liou, W.;Geuze, H.J.;Geelen, M.J.H.;Slot, J.W.; *'The Autophagic and Endocytic Pathways Converge at the Nascent Autophagic Vacuoles*', The jour. Of Cell Biology, **13(1),** 61-70(1997).

[20] Huang, S., Tsutsui, G., Sakaue, H., Shingubara, S. and Takahagi, T., Jpn. J.Appl. Phys., Part 2, **38(1998)**, L473.

[21] Murali Sastry, *'Phase transfer protocols in Nanoparticle Synthesis',* Current Science, **85(12),** 1735-1745(2003)

Chapter 3: Fabrication of Nanoparticle Arrays

3.1 Introduction

As stated in Chapter 1, molecularly protected nanoparticles(MPNs) possess certain unique properties which can be utilized for various applications in photonics and electronic device fabrication. However, an ordered and addressable assembly of MPNs is required for utilizing these nanoscale components. These assemblies may be in the form of monolayer (for storage media), patterned (for Light emitting diodes, nanoelectronics), multilayer (for solar cells) or dispersed in a matrix (for composites or electronic packaging). In the following paragraphs, various "bottom-up" approaches reported in literature for fabricating arrays of MPNs will be discussed.

Geirsig et al[1] have reported a method of forming a monolayer of Au MPNs using electrophoretic deposition on carbon film coated TEM grid. The phenomenon of electrophoresis can be used to attract charged nanoparticles on a surface. Pt MPNs have also been arranged using the same method by Teranishi et al.[2] In this method, the alkane thiol protected NPs are deposited over an anodic surface under relatively low potential difference. The advantage is that extremely regular structures can be formed rapidly, but the stability of these structures is poor since the particles are not truly adsorbed on the surface. Arrays can also be formed by appropriate surface functionalization of the substrate and placing it inside a solution containing colloidal MPNs for a predetermined period of time. Functionalized surface bears chemical groups which are capable of binding the colloidal particles either covalently or electrostatically. Based on the requirement either the MPNs or the substrate surface can be functionalized so that they have a strong affinity for each other. Shipway et al.[3] have reported various schemes for surface functionalization of substrates as well as MPNs. Doron et al[4] have reported monolayer formation of citrate stabilized Au MPNs on amine-functionalized and thiol-functionalized conducting glass (ITO) substrate. Multilayer assembly of nanoparticles can be formed using layer-by-layer (LbL) assembly method. In this method, monolayer formed is functionalized further so as to adsorb more nanoparticles. Fu et al[5] have

reported gold nanoparticle multilayer assembly by using UV irradiation to functionalize the monolayer formed. Fabrication of multilayer via alternating adsorption of positively and negatively charged species from an aqueous solution has also been reported[6] These multilayers can be used for a variety of applications like biosensors, photovoltaics, nanocomposites etc[7]**.** However, arrays formed by such techniques are not close packed due to the random nature of the adsorption process.

Evaporation driven self assembly (EDSA) is another method of forming arrays on a variety of substrates.[8] The simplest example of EDSA is casting a drop of a colloidal solution of nanoparticles on a flat surface and allowing the solution to evaporate slowly under controlled conditions[9,10]. The arrangement obtained depends on the concentration of the nanoparticles and their shape. If the concentration is high, we get ordered 3-D arrays or superlattices[11]. Under optimum conditions, as the solvent evaporates dense small monolayer islands are formed consisting of hexagonal packed domains. However, even a small surface irregularity or defect can cause nanoparticles to aggregate and cause contact line pinning due to hindrance in the movement of nanoparticles, leading to irregular deposition. A liquid-liquid interface has been employed to overcome this problem since it has an inherent uniformity in the lateral direction. Using hydrophobic MPNs dispersed in an organic solvent, one can produce islands of monolayers on water surface by EDSA. A Langmuir trough[10] can then be used to decrease the area available to the particle rafts thus bringing them closer to form dense monolayer, however, it may lead to the formation of multilayer. Santhanam et al[12] provided a viable solution to this problem by using a specially fabricated Teflon cell. The idea was to get a concave water surface so that the evaporation starts from the middle of the surface and proceeds towards the periphery. The hydrophobic nature of Teflon causes the water surface to take a concave shape. The organic solvent containing nanoparticles, dispensed over the surface is hydrophobic and forms a convex surface over water with Teflon. The self assembly starts from the middle of the liquid-liquid interface and if the concentration is large enough, monolayers are formed at the centre while excess MPNs move towards the periphery. Whenever a liquid–liquid interface is utilized, the monolayer formed needs to be transferred onto a solid substrate using Langmuir-Blodgett(LB) or Langmuir-Schaefer(LS) method[5,13]. In the former, the substrate is dipped into the water surface and

slowly withdrawn, perpendicular to the water surface, so that the MPNs get deposited over the substrate as the solvent evaporates. In the latter, the substrate is brought parallel to the water surface and pressed gently over it to transfer the film. This method was found suitable in situations where the substrate is hydrophobic. If it is hydrophilic then water will stick to the substrate hindering proper transfer of monolayer. Santhanam et al[14] developed a two step process for transfer of MPNs monolayer from the liquid surface to a solid substrate by using a PDMS(Polydimethylsiloxane) stamp as a carrier. Monolayer is first transferred to the PDMS stamp and then to the substrate by pressing the stamp gently on the substrate surface.

Direct coating techniques like spin-coating, dip-coating and spray-coating can also be classified under EDSA. Hong et al[15] have reported fabrication of Ag and Co NPs on Si and SiO_2 substrates by spin coating. Spin-coating technique can rapidly fabricate "uniform" nanoparticle assemblies over a large area on various kinds of substrate. However, the ordering of nanoparticles is still unsatisfactory and needs to be improved by controlling the drying process of the solvent during coating.

In addition to nanoparticle ordering, the patterning of arrays is also of paramount importance. Patterned nanoparticle structures can be used for various applications including nanoelectronic interfacing, sensors and in microfluidics to control chemical reactions on a micro/nano-scale[5,7]. To fabricate the patterned nanoparticle assembly, several methods have recently been developed. A soft lithography technique (microcontact printing: μCP) proposed by Whitesides et al.[16] has been utilized to form patterned nanoparticle arrays. Santhanam et al[14] have reported a combination of EDSA on water surface and μCP to obtain large areas of patterned arrays. Direct patterning of surfaces by scanning probe microscopy tools, such as by STM and AFM tips, is interesting but these are not cost effective and industrially feasible means. In this method, uniformly formed arrays are "swept" or etched using cyanide ions by touching it using an STM tip[17,18]. Dip pen lithography as proposed by Piner et al[19] can provide patterned arrays but being sequential, it is inherently a slow process.

Alternative approach is to adsorb nanoparticles onto a substrate that already bears a pattern. This pattern can be formed using photolithography based techniques. Irradiation at 254nm under air oxidizes the thiol functionalized surface to sulfonates,

which are unable to bind gold colloids.[3] Subsequent treatment of this surface with gold colloid solution results in nanoparticles adsorbing only at areas which have not been irradiated. Several biologically inspired methods have also been reported for patterning of nanoparticles on substrate surface[20]. As reported by Fu et al,[21] DNA based patterning can produce 1-D quantum dot of CdSe surrounded by Au nanoparticles. For array characterization, we need to observe the topography of the surfaces formed. Atomic Force Microscopy, gives the topography of the surfaces at the nanoscale and can be used to characterize the arrays formed. Besides this, Scanning electron microscopy (SEM), Transmission electron microscope(TEM) and X-ray diffraction (XRD) techniques can also be used for characterization.[3]

In the above paragraphs, we have reviewed some of the available techniques for making nanoparticle architectures. The key issue is to fabricate large area of nanoparticle arrays rapidly with regular features. In the present work, we have concentrated on the fabrication of nanoparticle arrays using EDSA over water surface. This method was chosen over its competing processes since it offers better control over the monolayers formed by manipulation of the concentration, and other experiment conditions.

3.2 Characterization and Analysis details

The characterization techniques used to analyze arrays are Transmission electron microscope(TEM), Atomic force microscopy(AFM), FTIR and UV-Vis spectroscopy Most commonly, TEM or Transmission Electron Microscope, is used to characterize the arrays. TEM utilizes electron beam instead of normal light as in the case of optical microscopes. Since electron beam has much lower wavelength, it is possible to get a resolution thousand times better than that of with a light microscope. Atomic Force Microscopy or AFM can also be used to characterize the area over which monolayer is formed but its resolution is not high as compared to TEM. AFM operates by measuring attractive or repulsive forces between a tip and the sample, where the tip is of the order of 5-100nm in width.(Appendix II) In the present chapter we will be discussing the TEM and AFM characterization results only.

TEM provides information regarding the packing of arrays while AFM gives the length scales over which the arrays are distributed uniformly. For preparing TEM samples, a carbon film coated copper TEM grid was dropped on the water surface and lifted carefully from one side using forceps such that the water drips from one side only. The MPN layer can also be lifted using a PDMS stamp and stamped on a clean silicon surface or Quartz plate for characterization by AFM, UV-Vis or FTIR. AFM analysis was performed on the silicon surface to assess the length scales over which the film was continuous. Quartz samples were used for carrying out UV and FTIR analysis.

3.1 TEM image analysis: A Foreword

The area over which the arrays are formed is in the range of square centimeter, while the area of a TEM grid is in the range of square millimeter. This grid is further divided into subsections of 100μm x 100μm each. This implies that while imaging we are viewing a very small part of the actual array. To assess uniformity, TEM samples were taken from two to three different spots of the array formed over the water surface. Also, while imaging, the images were taken from different spots, that were randomly chosen on the TEM grid.

The images obtained in TEM are gray scale images, darker at places through which the electrons can not penetrate through (eg gold nanoparticles). This image contains data regarding the particle size, packing density as well as the crystal structure. TEM Image analysis was done using ImageJ® software and in-house designed software using IGOrPro®. The above two softwares together with a MATLAB program (Appendix –IV) provide the information regarding the % of Area covered, distance between the particles, angular distribution between neighbouring particles and the particle size distribution. Thresholding of digitized image is an important consideration as it removes unnecessary disturbances created by small speckles etc on the carbon grid, but it may also affect the size significantly. The outline of the thresholded binary image was superimposed on the original image and observed visually to confirm proper thresholding. The thresholding parameters were varied till they passed the visual inspection test. An example of a superimposed image is shown in fig. 9.

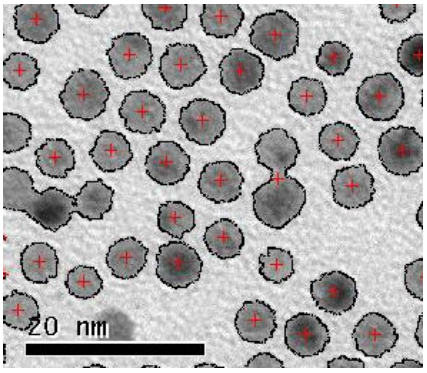

Figure 9: Threshold contours superimposed over original image to verify the quality of thresholding. The red '+' are the centroids of respective particles.

The parameters considered for analyzing the images included the % of area covered, size distribution, neighbouring distance and the angular distribution. An array can be termed as good if it has

- narrow particle size distribution
- Area coverage % is close to ideal value
- angular distribution centred around 60 degrees

For comparison, we need to define what can be called a "perfect or ideal array". A suitable definition will be an image having monodisperse particles regularly arranged in a hexagonally close packed structure. A hcp structure is considered ideal as the forces involved in the self assembly process are isotropic in nature. The distance between the particles varies as the capping molecule and the size of the particle changes. To get an idea of the inter-particle distances in ideal array, patches in the arrays fabricated were identified, where hexagonal close packing of monodisperse particles is visually observed. Fig. 10 shows examples of such regions in an array. The inter-particle distance were calculated for both 5 and 10 nm size range particles and based on that % area coverage for an ideal array was calculated. The distance obtained from three different spots were averaged.(table 5)

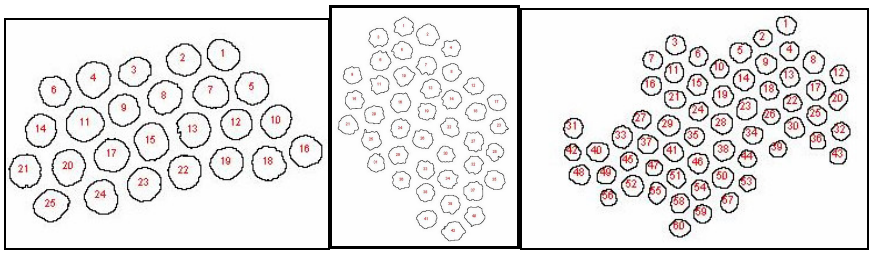

Figure 10: Example of places chosen for finding interparticle distances of the ideal array. The images only show the thresholded contours of the gold regions.

S. No.	Nominal Particle Size	Distance between particles(centre to centre) (mean±SD)	Ideal Surface coverage(for mean centre to centre distance)
1	5nm	7.2±0.30nm	43.8%
2	10nm	13.5±0.89nm	49.8%

Table 5: Experimental value of interparticle distance and computed ideal surface coverage of close packed sections

Note: Ideal surface coverage corresponds to the area covered by the gold nanoparticles only and does not account for the capping ligands which cannot be visualized in a TEM image.

3.3 Results and discussion

3.3.1 Ligand exchange reactions

Generally, nanoparticles synthesized generally have either electrostatic or steric stabilization. The stabilization or functionality of the nanoparticles can be tailored as per the end requirement using ligand exchange reactions. For the fabrication of arrays using self assembly over water surface, the requirement is that the particle should be easily dispersed in suitable organic solvents. The solvents are chosen based on their boiling point, density and miscibility with water. The requirements include, low boiling point to allow faster evaporation, lower density and immiscibility with water so that it floats over it. Based on these requirements, the solvent chosen was n-hexane and capping molecule was dodecanethiol. Gold nanoparticles were available synthesized via two sources,

namely the microemulsion route and tannic acid route. The former were stabilized by a layer of surfactant molecule, while the latter was electrostatically stabilized by citrate molecules. Capping of both with DDT was attempted and results are discussed below.

3.3.1.1 Capping of particles synthesized via Microemulsion method

Stable nanoparticles, synthesized via microemulsion route as described by Chiang et al[37], were available. It was speculated that, these nanoparticles could be used for making arrays, if we were able to cap them with a suitable ligand and isolate them. Briefly, the process for making the nanoparticles is as follows. A mixed reverse micellar solution of gold salt in isooctane with AOT and Brij30 was prepared and to this another mixed reverse micellar solution containing hydrazine hydrate was injected in equal volumes. The solution was stirred for 12 minutes. For capping we followed the process as explained by Lin et al[34] who report thiol capping of gold nanoparticles prepared by using CTAB as a surfactant.

A 1 ml aliquot of the gold colloid was taken and 0.5 ml of dodecanethiol was added to it. This solution was kept for two hours, which resulted in the change of colour from wine red to cloudy white. The solution was then centrifuged and precipitate kept overnight for drying. It was then redispersed in 5ml toluene by sonication for 30 minutes. The final solution obtained was pink in colour. Fig. 4 shows the UV-Vis spectra before and after capping of the particle solutions.

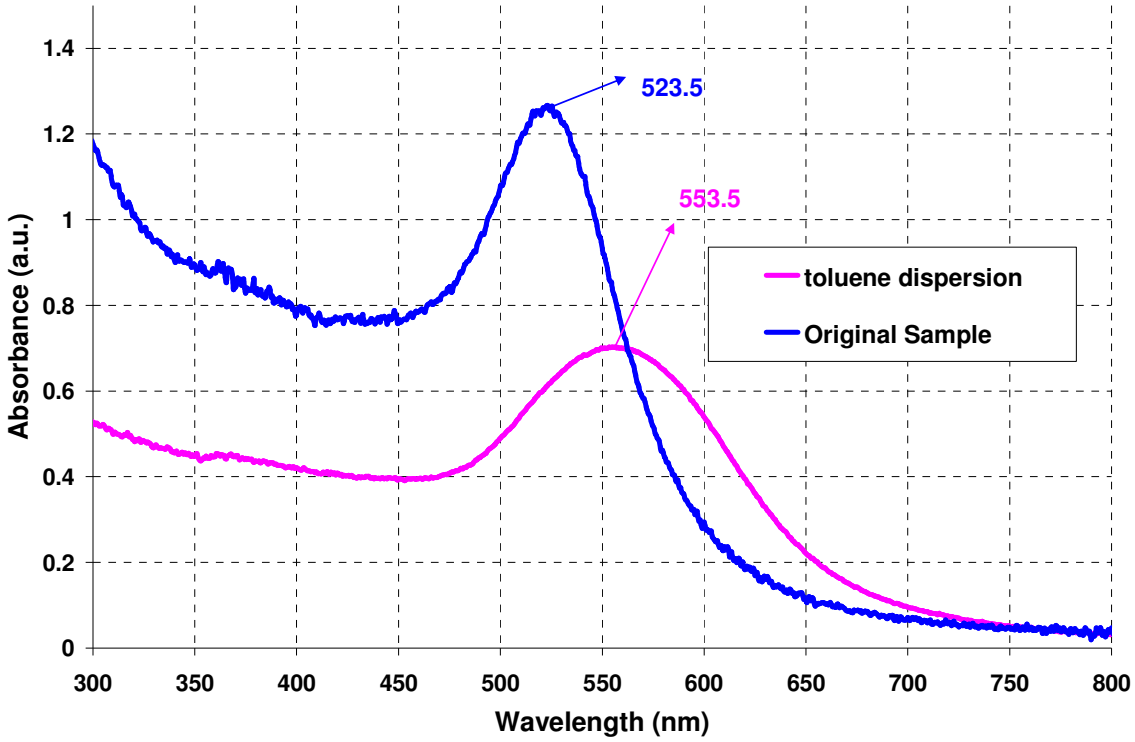

Figure 11: UV-Visible Absorption spectra of gold sol obtained from micellar synthesis before and after capping with DDT

As seen in fig. 11, the surface plasmon resonance peak shifts from 523.5nm to 553.5nm after capping. As stated previously, as the size of the nanoparticle increases the UV-Vis spectrum peak shows a red-shift i.e. towards higher wavelength. This implies that the capping process is causing an increase in the size of the nanoparticles. This is corroborated by DLS analysis of the samples which shows that the mean particle size before capping was 11.3±1.5 nm which changed to 26.2±1.2 nm after capping. Since we were not getting nanoparticles of the desired size ranges through this method, it was not pursued further.

3.3.1.2 Capping of particles synthesized via Tannic acid method

The nanoparticles synthesized as per the tannic acid route reported in the previous chapter are stabilized by electrostatic charge repulsion. Calculations reveal that the amount of DDT required to cap 5nm size particles synthesized from 0.01 gm of gold salt is equal to 0.3 µl while for 10 nm size particles it is approximately 0.6 µl (see Appendix-

III). Typically, we used some 100 times more than the calculated value to account for losses to walls of the beaker as well as for faster capping. Also since it is insoluble in water, ethanol was used as the mediating solvent. Typically, to cap 5 nm(or 10 nm) sized particles, 30 ml of ethanol was taken and 3 µl(or 6 µl) of DDT was added and mixed well. Then 30 ml of the gold colloid solution was added drop by drop to this while constantly stirring the mixture. The solution was kept for 10-12 hrs to allow the DDT to cap the particles and then centrifuged at 4000 rpm for 1 hour. The supernatant was carefully removed and the precipitate was washed twice with ethanol to remove any leftover DDT in the test-tube. The precipitate was then left for drying and redispersed just prior to casting arrays. A comparison of UV-Vis spectra before and after capping is shown in fig. 12.

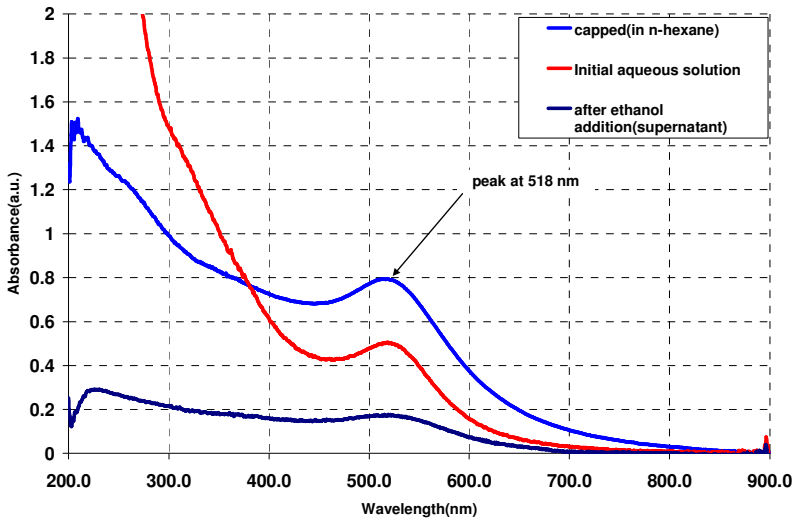

Figure 12: UV-Vis spectra of Aqueous Gold colloid(5nm size range) before and after capping

The samples after redispersion were analysed by DLS to get the size distribution. The results are shown in Table 6. It was observed that the 10 nm size range particles were not stable in hexane as compared to 5 nm which were quite stable. 10 nm particles agglomerated and settled down as soon as they are redispersed in any solvent. This caused problem in sizing them using DLS, because the count rates were not stable.

S. No.	Experiment details	Initial size(in aqueous solution)		Size after capping	
		Mean	Polydispersity	Mean	Polydispersity
1	With 3ml TA	7.1±0.90	12.7±3.45%	6.7±0.20	0.7±0.02%
2.	With 0.1ml TA	12.7±0.62	10.0±2.96%	--	--

Table 6: DLS data before and after capping with DDT

Another organic solvent, Dichloromethane, gave some stability to these particles but since its specific gravity is greater than water it was difficult to make arrays using it. It was necessary to identify some suitable solvent for redispersing these particles. Four different combinations of solvent were used and the time dependent UV-Vis spectra is shown in fig. 13. The combinations were chosen such that the boiling points are low, while the density of the mixture is less than water.

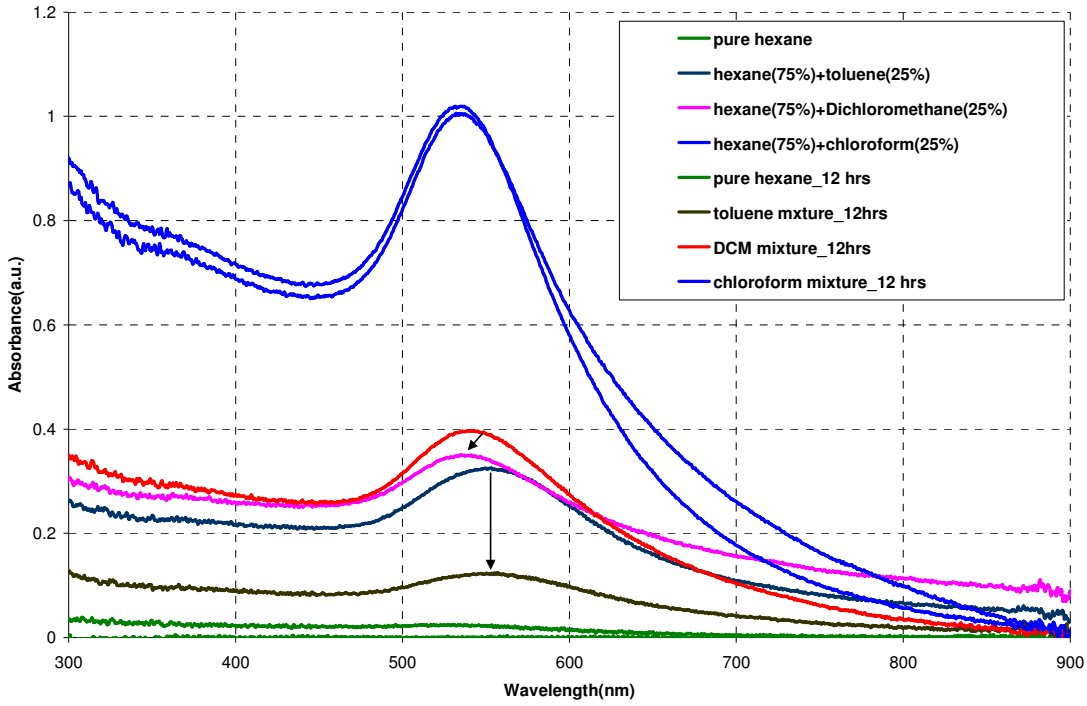

Figure 13: Exploring different solvents for dispersing 10nm size range particles

As observed from figure 13, the chloroform/hexane combination performs best as it shows lesser loss over a period of 12hrs as well as better surface plasmon resonance peaks signifying higher concentration of nanoparticles.

3.3.2 Fabrication of Arrays

After changing the surface functionality, the nanoparticles have a hydrophobic surface and can be easily dispersed in low boiling point organic solvents. These are the required conditions for self assembly over water; as the hydrophobic coating prevents the nanoparticles from dissolving in the aqueous sub phase. Low boiling point solvent was required as otherwise the amount of time required to evaporate will be more allowing the nanoparticles sufficient time to agglomerate in the solution and form multilayers instead of monolayers.

The process followed in general for fabricating arrays is as described by Santhanam et al[12]. The teflon cell was kept in a clean petridish. A special tripod was designed to adjust the level and it was made flat using spirit level. Water was slowly poured into it until the water level just touches the lower inside edge of the cell. This is the point when the water surface is pinned to the lower edge. Now the rate of addition of water is decreased to dropwise, and it is added till the required curvature of the water surface is obtained inside the cell. Visual aids, such as the curvature of tubelight reflections etc are used due to lack of more quantitative techniques to measure curvature.(see fig 14)

Figure 14: Teflon cell kept in a petridish.Note the reflection of tubelight marked by an arrow which was used to identify the right curvature(left); An image after the formation of self assembled MPN array on the water surface.(right)

Now solvent containing the nanoparticles is gently cast in the centre till it covers the whole of the water surface inside the cell. After this it was allowed to evaporate under desired conditions. During evaporation it can be covered with a hollow cylinder to avoid turbulent air *** that will disturb the ordering of the monolayer. Typical images of the experiment before and after fabricating MPN arrays are shown in fig 14. Depending on the solvent it requires around 3-6 minutes for the solvent to evaporate leaving behind layers of MPNs. The film adds a purple hue to the water surface after drying and has a reflective metallic sheen at the grazing angles..

The array formed is dependent on various factors like the concentration of nanoparticles, area over which the layer is formed, rate of evaporation of solvent etc. It was observed that the monolayer formed had irregularities at the boundaries. This was due to the instabilities that occur when the angle, which solvent makes with the Teflon cell goes above a certain threshold. To avoid it, a new design was proposed in which a wedge was introduced hoping that it will cutoff the receding solvent contact line before it goes into the region of instability. The schematic of the design is shown in fig 15.

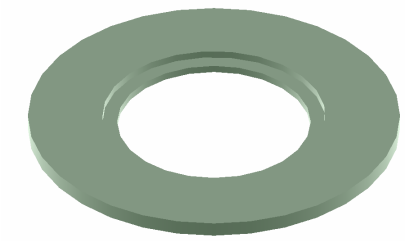

Figure 15: Schematics of Teflon cell with wedge

Three different cell designs along with one without any wedge were used. The description of cell designs used is given in Table 7. Wedge height was varied to avoid any overflow of the nanoparticle solution while array fabrication.

ID	Internal		Wedge		Remarks
	Diameter(mm)	Thickness(mm)	Diameter(mm)	Height(mm)	
CD1	20	2	--	--	*from ref 12*
CD2	20	0.6	24	1	
CD3	25	1	32	1.5	
CD4	26	2	30	1.5	

Table 7: Details of the Teflon Cells used for experiments

A few experiments were conducted to determine the effect of particle concentration, cell design used and the solvent evaporation rate. A brief description of the experimental conditions used is given in Table 8. Particle concentration was calculated based on the initial amount of aqueous colloid taken for capping with DDT. A important point to mention here is that since there can be a loss of nanoparticles during the experimental steps and the amount of nanoparticles may vary from test tube to test tube(within a batch), the particle concentration calculated is only approximate.

S.No	Particle size range	cell used	solvent	Concentration of particles(per ml)	Remarks
1	5nm	CD3	Hexane	5.65E+13	
2	5nm	CD1	Hexane	9.04E+13	
3	10nm	CD1	DCM	--	*particles settled*
4	5nm	CD4	Hex+DCM (1:1)	1.59E+14	
5	5nm	CD1	" "	1.33E+14	
6	10nm	CD1	hex+CFM (3:2)	1.20E+14	
7	5+10nm	CD1	Hex:CFM (1:2)	--	
8	5nm	CD1	Hexane	2.82E+13	*T = 10^{o}C*

Table 8: Experimental condition for fabricating arrays

*** DCM: Dichloromethane; CFM: Chloroform; Hex: n-hexane*

Results indicate that the concentration and the area of the water surface used for fabricating monolayers plays a key role in the ordering of the particles. In cell CD3, the area was large also the distance between the edge and inner diameter and the outer diameter is large and most of the particles were seen to move towards the Teflon wall before the solvent evaporated completely. This is due to the hydrophobic nature of Teflon and its affinity with the DDT molecules capping the nanoparticles. The TEM images show that the arrays formed have sub-monolayer coverage. The coverage in terms of % area occupied by gold core is 29.8%, which is quite less when compared to the ideal coverage of 43.8%.

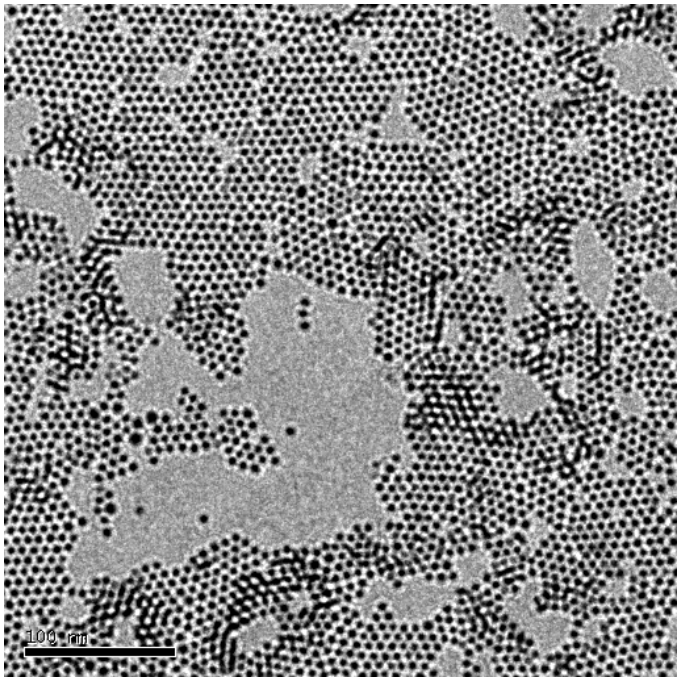

Fig 16(a):
Area % = 29.8%
Particle size: 5.2±0.62
Scale bar: 100nm

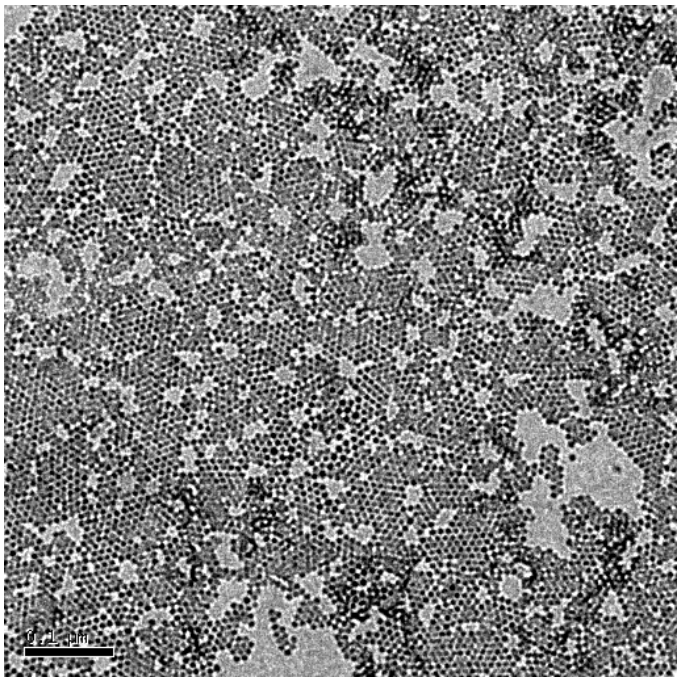

Fig 16(b):
Area % = NA
Particle size: NA
Scale bar: 100nm

Figure 16 : TEM images: 5nm nominal size, [solvent: n-hexane], [cell used: CD3] , [Particle concentration: 5.7e+13 per ml], 17(b) not analysed quantitatively since it was not focused well.

In the next trial the concentration of the nanoparticles was increased and the cell CD1 was used, which has a lesser area as compared to other cells. The monolayer formed in this case was quite ordered and lesser holes were observed. The coverage also increased to 36%.

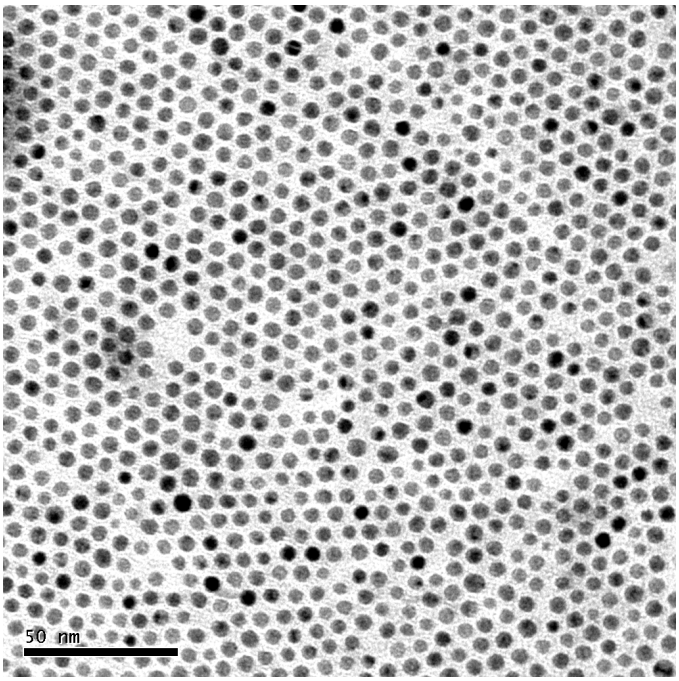

Fig 17(a):
Area % = 38.8%
Particle size: 4.9±0.61
Scale bar: 100nm

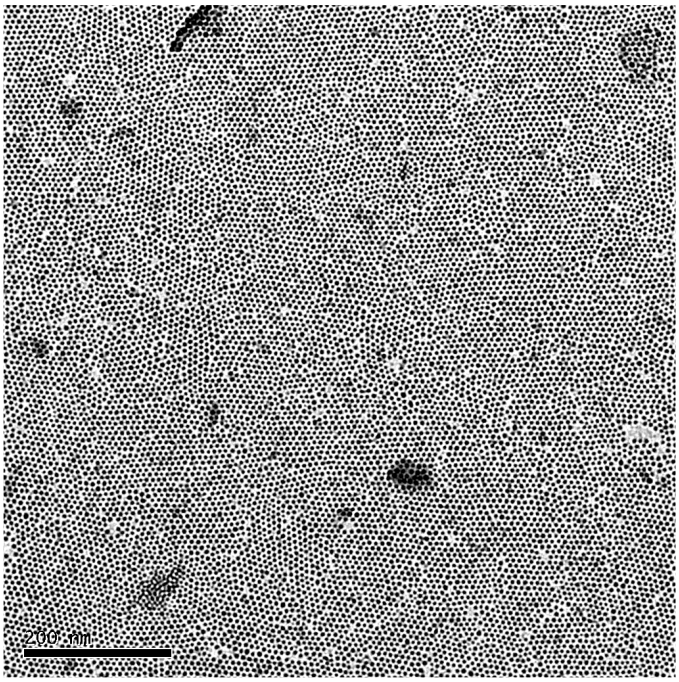

Fig 17(b):
Area % = 41.7%
Particle size: 5.4±0.63
Scale bar: 100nm

Figure 17 : TEM images: 5nm nominal size, [solvent: n-hexane], [cell used: CD1] , [Particle concentration: 9.1e+13 particles/ml].

The above two experiments were done with NPs of size 5nm. The TEM image analysis also confirmed the size of the particles to be 4.9±0.61 nm and 5.4±0.63 nm respectively.

An experiment was carried out using nominally 10 nm size particles. As mentioned earlier, it was observed that they were not stable in many solvents, hence the solvent used in this case was dichloromethane in which some stability was observed. Although the density of dichloromethane(1.322) is higher than water, yet we were able to evaporate it over the water surface. The results show very polydisperse particles and predominantly a multilayer formation. This may be due to the fact that the particles are not stable in the solvent and also as the Van der Waals force of attraction between them is larger while the steric hindrance insufficient, they prefer to form 3D superstructures, instead of a monolayer.

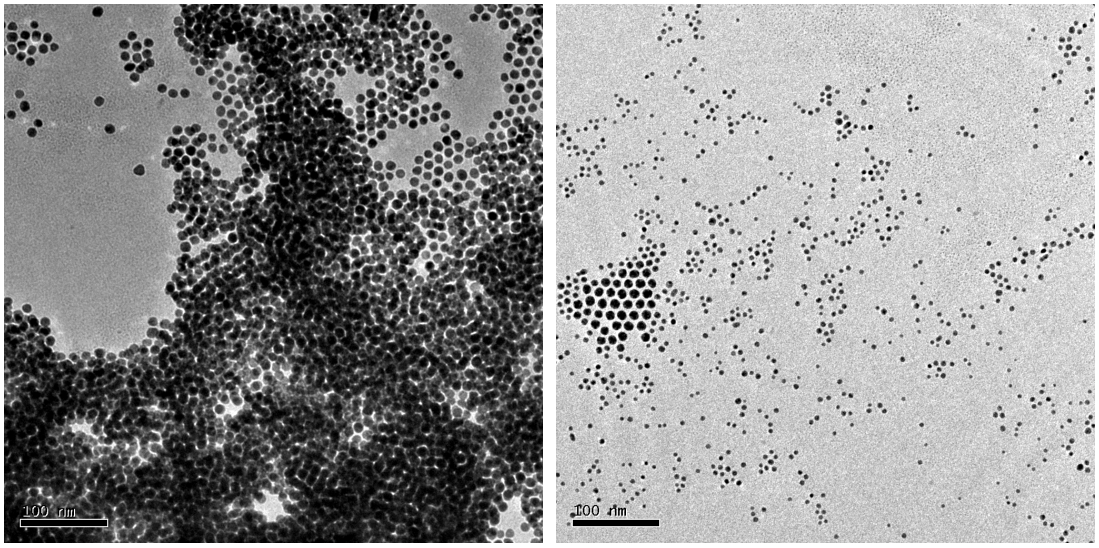

Figure 18: TEM images: 10nm nominal size, [solvent: Dichloromethane], [cell used: CD1] , [Particle concentration: NA(settled)]

In order to overcome this problem, the solvent was changed to a mixture of chloroform and n-hexane (1:2). The TEM images obtained still show patches of monolayers and multilayers. The monolayers formed are having an area coverage of 41.4%.

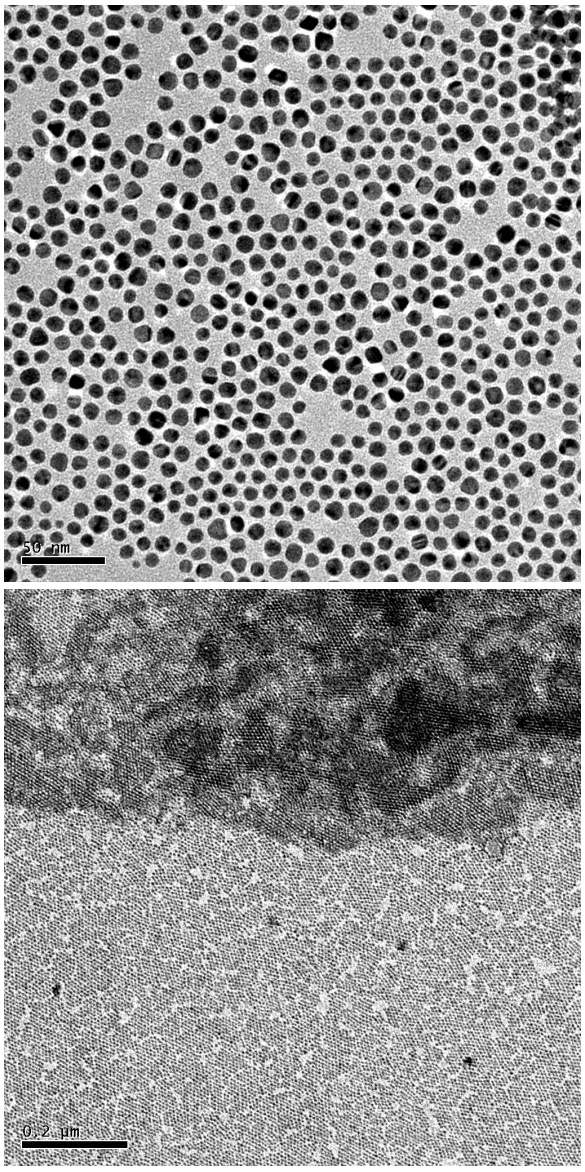

Fig 19(a):
Area % = 41.4%
Particle size: 9.4 ± 1.10
Scale bar: 50nm

Fig 19(b):
Area % = NA
Particle size: NA
Scale bar: 200nm

Figure 19: TEM images: 10 nm nominal size, [solvent: n-hexane+chloroform(1:2)], [cell used: CD1] , [Particle concentration: 1.2e+14 particles/ml]. Multilayers are observed alongwith monolayers in 19(b).

To observe the changes in the packing with solvent or evaporation rate, a mixture of hexane and dichloromethane(DCM) was used. Owing to its low boiling point, DCM increases the evaporation rate and hence the time of formation of arrays. Experiment was performed with 5nm size particles with equal concentration in two different cells CD1 and CD4. CD4 includes a wedge, but the dimensions of the wedge are decreased as compared to CD3. This was to decrease the loss of nanoparticles

observed in the first experiment. The arrays formed looked similar and have submonolayer % of area covered, namely 35.6% and 34.5% for larger and smaller area respectively.

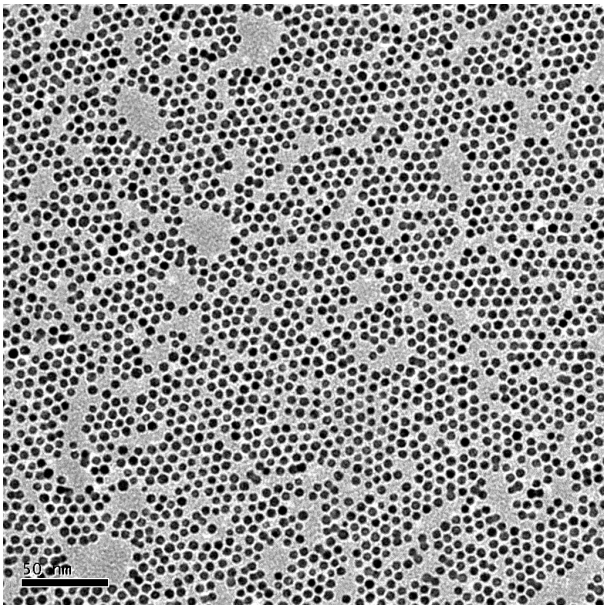

Fig 20 (a):
Area % = 39.9%
Particle size: 5.1±0.47 nm
Scale bar: 50 nm

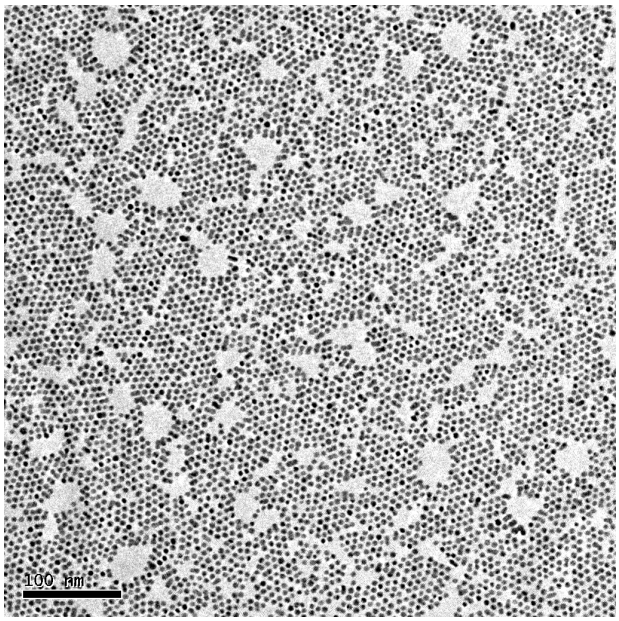

Fig 20(b):
Area % = 35.7%
Particle size: 5.2±0.66 nm
Scale bar: 100nm

Figure 20: TEM images: 5 nm nominal size, [solvent: n-hexane+dichloromethane(1:1)], [cell used: CD4] , [Particle concentration: 1.6e+14 particles/ml].

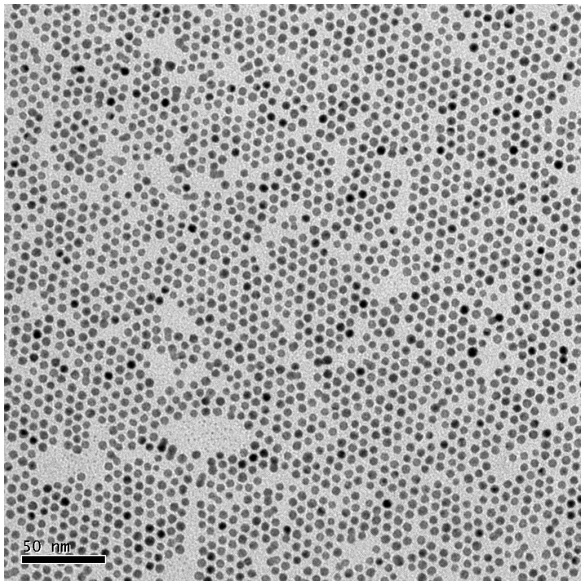

Fig 21 (a):
Area % = 36.3%
Particle size: 4.9±0.44 nm
Scale bar: 50 nm

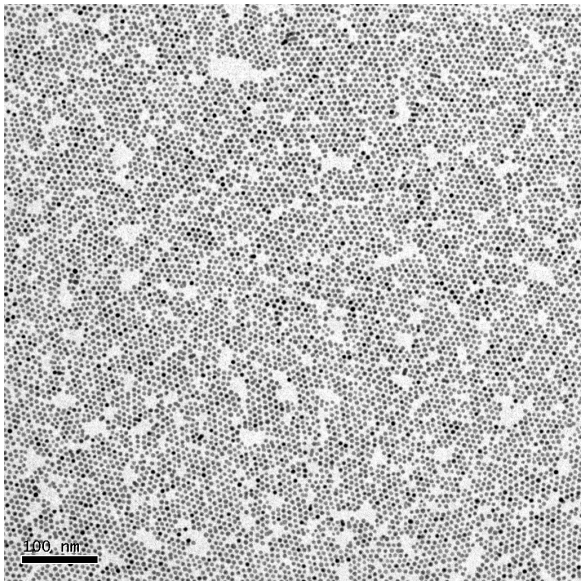

Fig 21 (b):
Area % = 34.5%
Particle size: NA
Scale bar: 100 nm

Figure 21: TEM images: 5 nm nominal size, [solvent: n-hexane+diclhoromethane(1:1)], [cell used: CD1] , [Particle concentration: 1.33e+14 particles/ml].

It was also speculated that low temperature will decrease the local fluctuations at the surface thus causing lower film breakage and grain boundaries. Hence, an experiment was performed with the water temperature around 10^{o}C. Initially, water taken from a refrigerator was at 5^{o}C, while the temperature at the end of the experiment,(after 6 minutes), it was 13^{o}C. The TEM image analysis shows that the % of area covered is 32.5% which is much less as compared to the previous

experiments. The reason may be due to longer time of evaporation, the particles moved towards the Teflon walls decreasing the overall concentration as well as they had enough time to get agglomerated and form superstructures. Also since the temperature was not constant during the experiment, water surface may have expanded, due to the rise in temperature, causing fluctuations at the nanoscale and breaking the monolayer. Further experiments with a chamber maintained at low temperatures are needed to confirm this hypothesis.

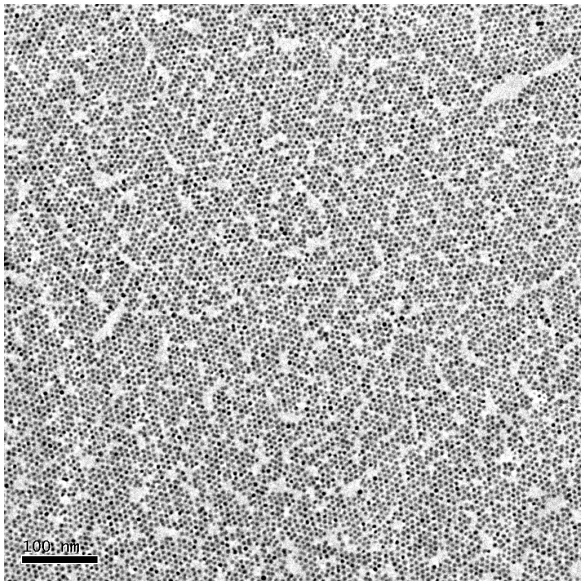

Fig 22(a):
Area % = 37.5%
Particle size: 5.52±1.06
Scale bar: 100nm

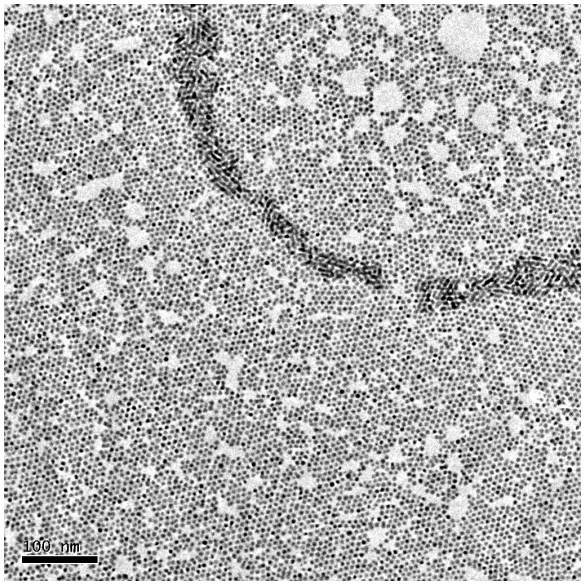

Fig 22(b):
Area % = NA
Particle size: NA
Scale bar: 100nm

Figure 22: TEM images: 5 nm nominal size, [solvent: n-hexane], [cell used: CD1] , [Particle concentration: 2.82e+13 particles/ml]. The experiment was conducted at low temperature.

An experiment to observe the ordering of a mixture of nanoparticles of 5nm and 10nm nominal size was conducted. the concentrations used were equal in terms of number of nanoparticles per ml. as seen from the TEM images, very less 10nm size particles were observed and the mostly the array was composed of 5 nm size range particles.

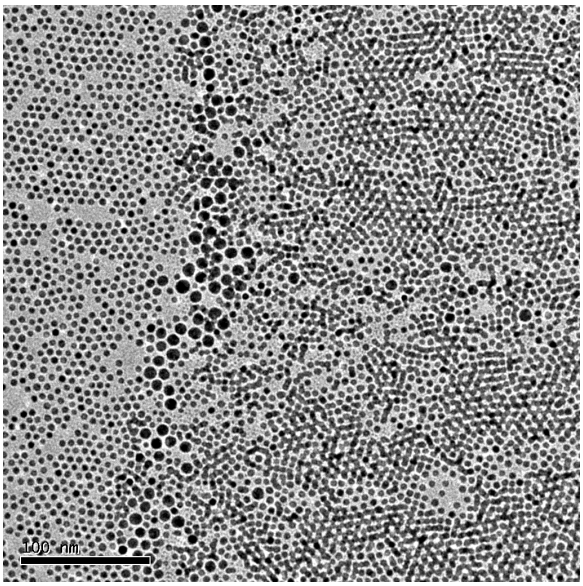

Fig 23 (a):
Area % = NA
Particle size: NA
Scale bar: 100 nm

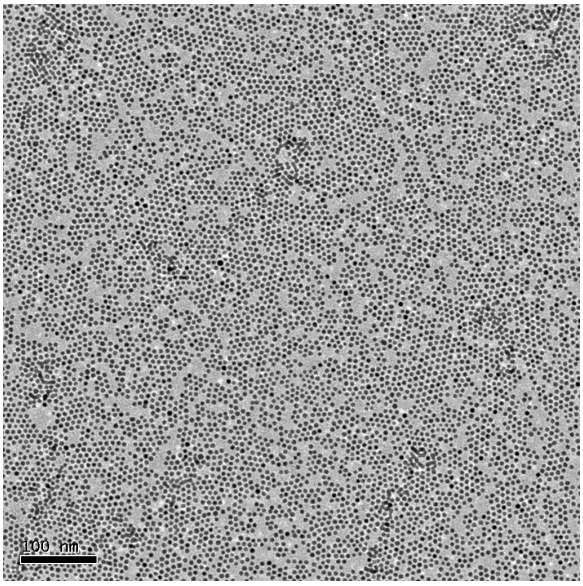

Fig 23 (b):
Area % = 32.13
Particle size: NA
Scale bar: 100nm

Figure 23: TEM images: 5nm+10nm nominal size, [solvent: n-hexane], [cell used: CD1], [Particle concentration: 9.1e+13 particles/ml]. Mixture of particle sizes of 5nm and 10nm range. (above) Shows the presence of 10nm but most of the spots they were absent in other images.

AFM was used to characterize the length scale over which the arrays are distributed uniformly. The advantages of AFM characterization over TEM is that it gives the topography of arrays over larger area as compared to TEM which gives a more localized view. The arrays formed were stamped on a clean Silicon wafer(surface roughness<1nm) using PDMS stamp. For cleaning the wafer, it was first sonicated in toluene, then in acetone and finally in methanol and dried in the laminar hood. Surface roughness was calculated by scanning an area of 5μm x 5μm, in tapping mode at 3 different locations over the surface.

The diameter of the AFM tip is in the range of 30nm when unused and increases as it is being used due to wear and tear. Since the gap in between the particles in close packing is of the range of 2-4 nm, tip cannot reach in between the particles and will continue to image the topography from the top only. To analyse, therefore, we need to have or create a hole in the array big enough for the tip to penetrate and image. To do this, tip was moved over the array surface in contact mode with a force equivalent to 150 nN. This force is sufficient to scratch and remove the nanoparticles from the surface without scratching the silicon surface. After this, imaging was done in tapping mode over a larger surface area.(Fig. 16)

As observed in the image, the place where the surface was scratched is 6 nm lower as compared to the other places. This means that the array formed is of height ~6nm which is expected since we used nominally 5nm size particles to fabricate it and also corroborates the DLS results(6.7±0.20 nm).

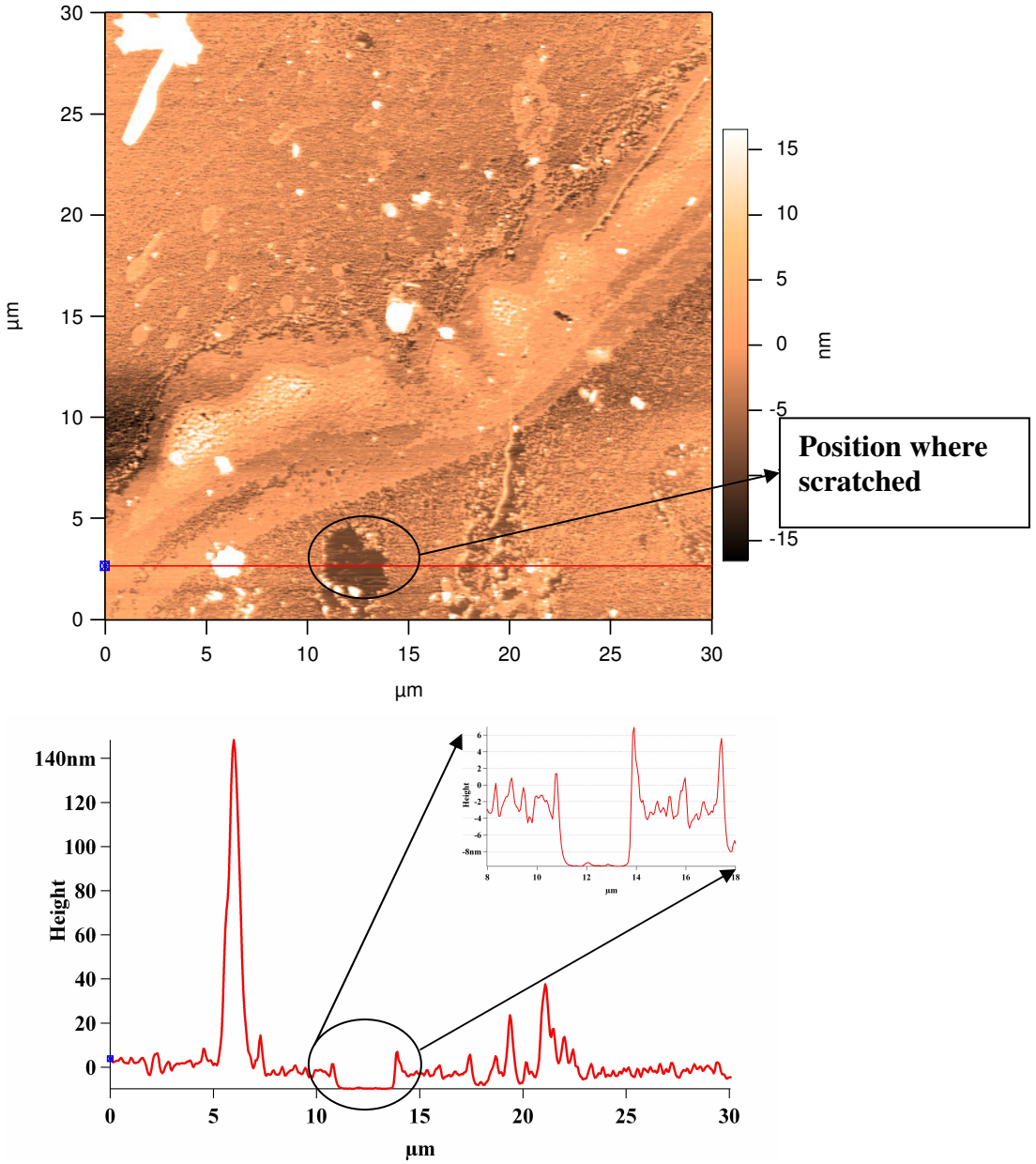

Figure 24: AFM images of array stamped over Silicon substrate.(above) The red line in the figure is the place where the cross-section is taken and depicted in the figure below.

3.4 Conclusions

Ligand capping of gold nanoparticles obtained via microemulsion and tannic acid route was carried out. Desired size ranges were obtained from the latter were used for making arrays using self assembly over a curved water surface. It was observed that the quality of the arrays obtained are a function of concentration of nanoparticle used as well as solvent evaporation rate. More uniform arrays are obtained at faster evaporation rates. It was also observed that the cell designed with a wedge, was not successful in limiting the instabilities while drying was not very successful and resulted in greater loss of particles to Teflon surface as compared to the original one.

References

[1] Giersig M; Mulvaney, P., *'Preparation of ordered monolayers by electrophoretic deposition*', Langmuir, **9(12),** 3408 (1993)

[2] Teranishi, T.; Hosoe, M.; Tanaka, T.; Miyake, M.; *'Size Control of Monodispersed Pt nanoparticles and their 2D organization by Electrophoretic deposition'* , *J. Phys. Chem.,* **103,** 3818 - 3827 (1999)

[3] Shipway, A.N.; Katz E.; Willner, I., '*Nanoparticle Arrays on surfaces for electronic , optical and sensor application',* ChemPhysChem**, 1**, 18-52 (2000),

[4] Doron, A.; Katz, E.; Willner I., *'Organization of Au Colloids as Monolayer Films onto ITO Glass Surfaces: Application of the Metal Colloid Films as Base Interfaces to construct Redox-Active Monolayers,* Langmuir, **11**, 1313-1317 (1995)

[5] Fu Y.; H. Xu; S. Bai; D. Qiu; J. Sun; Z. Wang; X.Zhang, *'Fabrication of a stable polyelectrolyte/Au nanoparticles multilayer film'*. Macromol. Rapid Commun. **23**, 256–259, (2002)

[6] Hammond, P.T., *'Form and function of multilayered assembly: New application at the nanoscale*'. Adv Mater.*,* **16**, 1271 (2004)

[7] Maenosono, S.; Tatsuya, O.;Yukio Y.;'*Overview of nanoparticle array formation by wet coating'* ,J Nanoparticle Res*,* **5,** 5–15,(2003).

[8] Jaeger, H.M., *'Kinetically driven self assembly of highly ordered nanoparticle monolayers*', Nature mater, **5**, 265-270, (2006)

[9] Andres, R.P., *'Self Assembly of a two-dimensional super lattice of molecularly linked metal clusters'*, Science, **273**, 1690, (1996).

[10] Takayuki T.;Huang, S.; Gen T.; Hiroyuki, S.; Shoso S.; *'Fabrication of Two & Three-dimensional structures of nanoparticles using Lb method & DNA hybridization',* Proc. of Mater. Res soc. Symp, **702**, (2002)

[11] Whitesides, G.M.; Grzybowski, B., *'Self Assembly at all scales*', Science **295,** 2418-2421 (2002).

[12] Santhanam, V.; Liu, J.; Agarwal, R.; Andres, R.P.; *'Self assembly of uniform monolayer arrays of nanoparticles' ,* Langmuir, **19(19)**, 7881 (2003).

[13] Fendler J.H.; *'Self-assembled nanostructured materials*'. Chem. Mater. **8**, 1616–1624, (1996).

[14] Santhanam V.; Andres, R.P., *'Microcontact printing of uniform nanoparticle arrays'*, Nano Letters, **4(1)**, 41-44 (2004)

[15] Hong Y.K.; Kim, H.; Lee, G.; W. Kim,; Park, J.I.; Cheon, J.; Koo, J.Y.; '*Controlled two-dimensional distribution of nanoparticles by spin-coating method*', Appl. Phys. Lett. **80**, 844–846 (2002).

[16] Whitesides G.M.; Ostuni,E.; Takayama, S.; Jiang, X.Y.; Ingber, D.E.; *'Soft lithography in biology and biochemistry'*, Annu. Rev. Biomed. Biochem. Eng.,**3**, 335–373, (2001).

[17] Resch, R.; Baur, C.,;Bugacov,A.; Koel, B.E.; Madhukar, A.; Requicha A.A.G.; Will, P., *'Building and manipulating three-Dimensional and linked structures of nanoparticles using Scanning Force Microscopy*',Langmuir, **14(23)**,6613-6616 (1998).

[18] Doron, A.; Joselevich, E.; Schlittmer, A.; Willner, I.; *'AFM characterization of the structure of Au-colloid monolayers and their chemical etching'*, Thin Solid Films **340,** 183-188(1999).

[19] Piner R.D.; J. Zhu,;F. Xu;S.H. Hong; C.A. Mirkin, *'Dip-pen nanolithography*', Science, **283**, 661–663,(1999).

[20] Seeman, N.C.; Belcher, A.M., '*Emulating biology: building nanostructures from the bottom up*', Proc Natl Amer Soc, **99(2),**6451-6455 (2002).

[21] Aihua Fu; Christine, M.; Cha, J.; Hauyee, C.; Yang, H.; Alivisatos, A.P.; *J Am Chem Soc,* **126**, 10832-10833 (2004)

Chapter 4: Ligand removal

4.1 Introduction

A fundamental requirement for VLS-based nanowire growth is the presence of a metal particle acting as catalyst for anisotropic crystal growth. As observed in in-situ TEM images taken during growth, the wires have gold sticking to their growing tip.[1,2] This deposition of catalyst has been achieved via a variety of techniques like Laser ablation, thin film evaporation, gold colloid adsorption etc.[3] All of the reported methods result in a non-uniform distribution of particles and hence the wires grown are also not distributed uniformly. In the previous chapter a process of fabricating arrays of MPNs is described. The uniformity and order obtained could be used for further processing of nanowires or other application involving gold as catalyst if we can remove the ligand coating of the MPNs. The need to remove them is due to the fact that at reaction temperature, they melt and allow the gold cores to coalesce and then the ordering is also lost. Hence our next target is to remove these ligands without disturbing the lateral arrangement of the nanoparticles.

The ligand removal involves the breakage of bond, which in turn requires energy to be provided. Energy can be provided in the form of heat but since the particles are not adhering to the surface by any bond, they move after the melting of alkanethiol SAMs and will coalesce. Plasma etching, which is used in Silicon chip manufacturing industry to clean the substrate from organic impurities, can be a viable solution to this problem. Spatz et al[4] have reported the removal of block copolymers of polystyrene-*block*-poly(2-vinylpyridine) (PS-*b*-P2VP), using oxygen plasma, from the surface of gold nanoparticles.

Plasma, usually considered as a distinct state of matter, is basically an ionized gas composed of ions, electrons and other neutral species.[6] The plasma process is typically maintained by the use of a low pressure, radio frequency(RF) induced gaseous discharge. A carrier gas is introduced into a chamber maintained at low pressure, and RF power is coupled to it. This excites the carrier gas molecules and dissociates it into chemically active species. These species bombard the specimen kept into the chamber and depending on the gas used, cause physical damage (sputtering) or chemically react with the target molecules. The combustion products are carried away in the gas stream. The unique property of this process

is that it occurs at relatively low temperatures. By optimizing the experimental conditions for etching, amount of thiol being removed can be controlled. Also, during the process the temperature ranges reached are not very high (30-70^{o}C)[5], thus reducing the probability of particle coalescence. However, a critical issue in preventing coalescence is the ion bombardment energy that in turn is controlled by Plasma processing parameters, such as RF Power used, gas pressure, composition of gas etc.

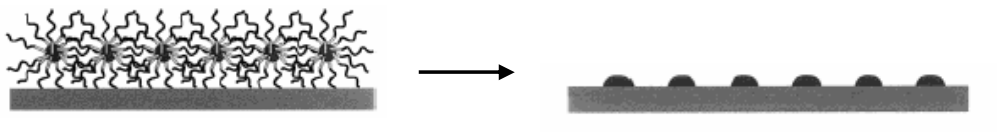

Figure 25: Schematic of the process of removal of ligands and formation of gold nanodots

4.2 Experiment and analysis description

The arrays were subjected to different plasma conditions to arrive at the optimum parameters to remove the ligands. TEM, contact angle and UV-Vis and FTIR spectroscopy techniques were used to characterize the arrays formed and the removal of ligands(see Appendix II for description of the techniques). Arrays fabricated as discussed in Chapter 2&3, are composed of MPNs and can be transferred to a TEM grid as well as a PDMS stamp using the Langmuir-Schaefer technique[7]. In this technique, the grid/PDMS stamp is brought into contact with the water surface horizontally and lifted carefully from one end. Once transferred to a PDMS stamp, arrays can be stamped on any substrate including Silicon wafer(for AFM measurements) or Quartz plate(for contact angle, UV-Vis and FTIR spectroscopy) by placing it in contact with the substrate.

GATAN plasma etching instrument(Solarus Model 950) was used for plasma treatment of arrays. The instrument has a specially designed sample holder that can handle TEM samples, while larger samples(quartz or silicon) can be inserted in another chamber. The gas used was a mixture of O_2 and H_2 with flow rates of 6.4 sccm and 27.5sccm respectively. This composition was recommended by the manufacturer for cleaning TEM samples and is claimed to induce low temperature rises, and low sputtering damage on the samples.

For TEM analysis, 2-3 different spots were randomly chosen on the grid using TEM analysis software and images were obtained at various magnifications at these spots before and after Plasma treatment. TEM image analysis was done using in-house developed software(IGORPro), ImageJ and Clemex Vision PE software. In this case also, the boundaries of thresholded images were superimposed over the original image to observe the quality of thresholding. In order to quantify the data obtained from TEM images in terms of coalescence versus the plasma power, we used the number of features as the criterion. For a similar magnification image, the ratio of the number of features before and after plasma was plotted against the plasma power used to etch.

The contact angle is another way of analyzing the extent of removal of ligand molecules. The contact angle is the angle at which a liquid/vapor interface meets the solid surface.[8] The contact angle is specific for any given system and is determined by the interactions across the three interfaces. Using water as the liquid, an estimate of the hydrophobicity of the surface could be measured. In the arrays fabricated, Dodecanethiol(DDT) molecules, capping the nanoparticles, have $-CH_3$ groups protruding out, rendering the array surface hydrophobic. If all the DDT molecules are removed then the contact angle should decrease since gold and quartz surface exposed are hydrophilic. The contact angle of a surface having different domains can be predicted by Cassie equation(1) or by Israelachivli & Gee equation(2).

$$\cos\theta = \phi_1 \cos\theta_1 + \phi_2 \cos\theta_2 \text{ ……..…(1)}$$

$$(1+\cos\theta)^2 = \phi_1((1+\cos\theta_1)^2 + \phi_2((1+\cos\theta_2)^2 \text{ ……(2)}$$

where θ = contact angle of the whole surface

ϕ = the surface fraction in terms of area

1,2 subscript for different type of surfaces

Eqn. 1 is valid for larger domains while eqn. 2 predicts better results when the domains reach the molecular dimensions. Contact angle of water droplet(3 μl) was measured at five-six different locations over the array surface using the sessile drop method and averaged out. A Rame-harte Goniometer was used for taking measurements. For UV-Vis spectroscopy measurements, the quartz substrate was kept in the path of the beam by using adhesive tapes. FTIR measurements were also taken for arrays stamped over quartz substrates to confirm the presence of DDT molecule.

As reported by Spatz et al,[4] for removing diblock copolymers of PS-*b*-P2VP, the particles were exposed to 100W plasma power with pure O_2 gas for a time period of 10 minutes. In our case, the surfactant chain molecules are much smaller as compared to these polymers. Hence, the power was varied from 50W to 10W, while processing time was varied from 40 sec to 10 sec. It was also possible to sub-divide the plasma exposure time into smaller intervals and to allow rest periods to prevent heating of the samples. The details of the experiment parameters used are given in Table 9. The results and their analysis details are discussed in subsequent sections.

S. No.	Sample ID	Size range	Power	Duration	Distribution of plasma power*
1	AS213	5nm	50W	30sec	single
2	AS5nm1	5nm	20W	40sec	15<20>15<20>10
3	AS5nm2	5nm	20W	30sec	single
4	AS5nm2_2	5nm	20W	20sec	10<30>10
5	AS5nmLT	5nm	20W	15sec	5<15>5<15>5
6	AS5nmmix	5nm	20w	10sec	5<15>5
7	AS10nm3	10nm	10W	20sec	10<30>10
8	AS10nm3_1	10nm	50W	30sec	10<30>10<30>10
9	AS10nm1	10nm	50W	15sec	5<15>5<15>5
10	AS10nm2	10nm	50W	10sec	5<15>5

Table 9: Experimental condition for Plasma etching

**the distribution plasma power is: cleaning time<rest time>cleaning time; single implies no rest time*

4.3 Results and Discussions

4.3.1 TEM Image analysis

As discussed earlier, plasma treatment was done to remove the ligand covering of the nanoparticles without disturbing their lateral arrangement. Optimization of treatment

parameters for both 5nm and 10 nm size range particle arrays was carried out. Starting from extreme conditions, the severity of conditions was decreased in steps. The first experiment was conducted with arrays of nominally 5 nm size particles with a plasma power of 50W and exposure time of 30 seconds. TEM images before and after treatment are shown in figure 18. It is observed that after treating with plasma, the order of arrays is totally lost and most of the particles have coalesced.

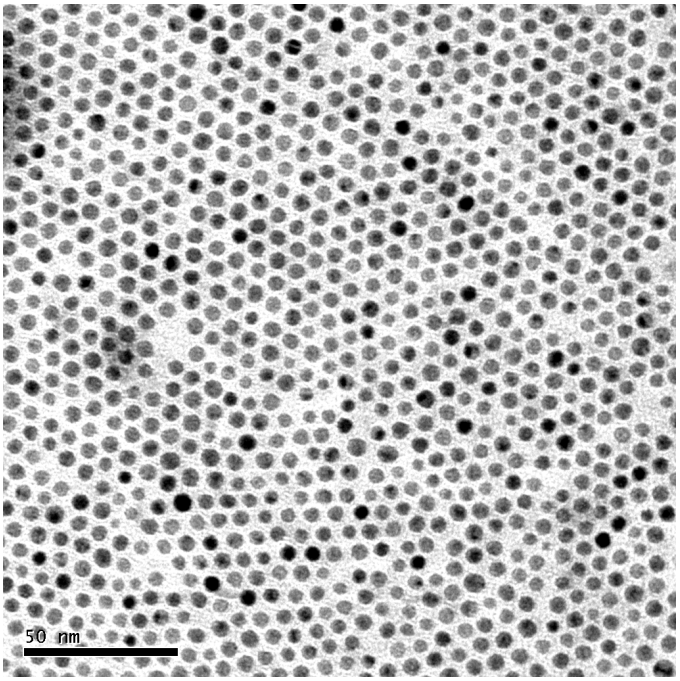

Fig 26(a):Before treatment
Area %: 38.8%
Feature count: 963
Magnification: 75000X

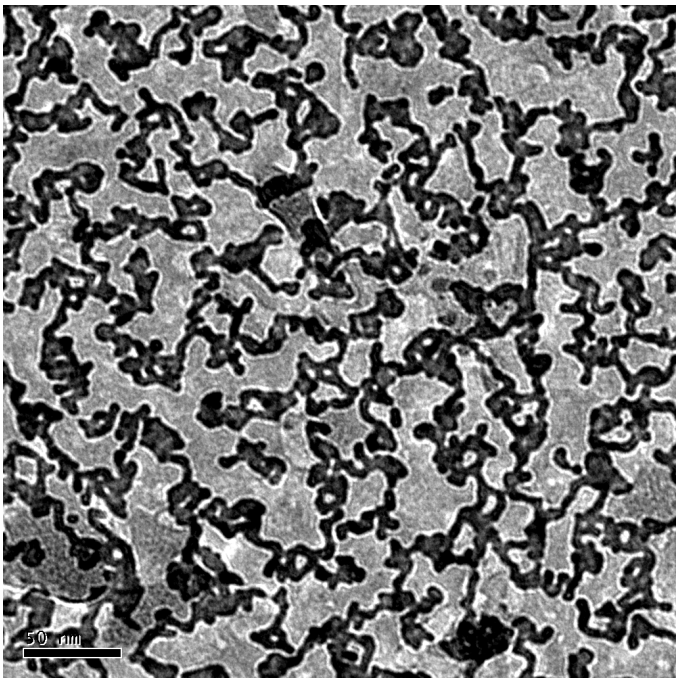

Fig 26(b): After treatment
Area %: 38.8%
Feature count: 52
Magnification: 49000X

Figure 26: TEM images: 5 nm size range [Plasma : 50W RF power], [exposure time:30sec]

There can be various reasons possible for the coalescence. It can be due to the movement of the nanoparticles due to ion bombardment(sputtering) resulting in coalescence due to van der waals attraction at small separation. Further experiments were conducted at a much lower Plasma power(20W) and the exposure time was varied from 40 seconds to 10 seconds. The results are shown in figure 27.

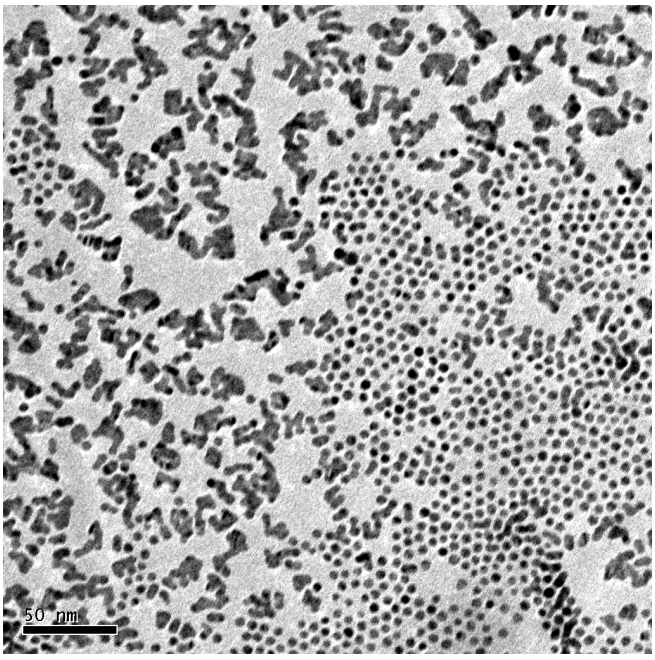

Fig 27(a):
Plasma : 20W RF power
Exposure time:40sec
Area %: 39.0%
Feature count: 867
Magnification: 49000X

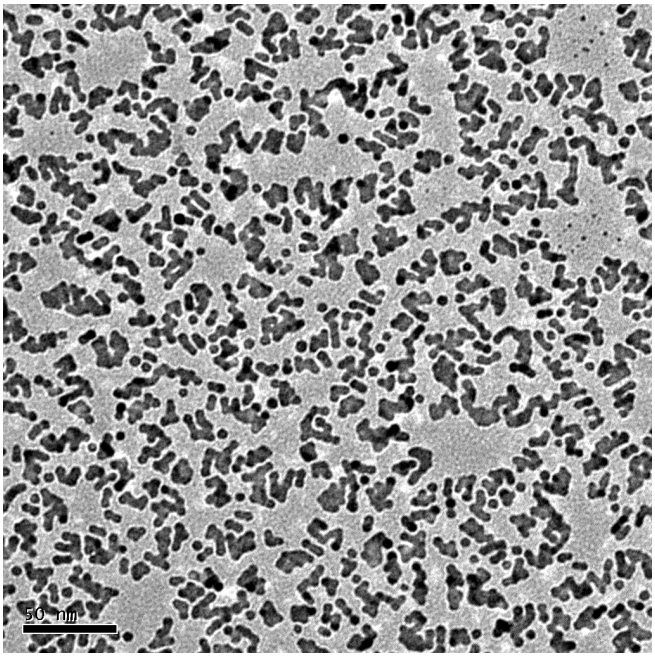

Fig 27(b):
Plasma : 20W RF power
Exposure time:30sec
Area %: 39.8%
Feature count: 512
Magnification: 49000X

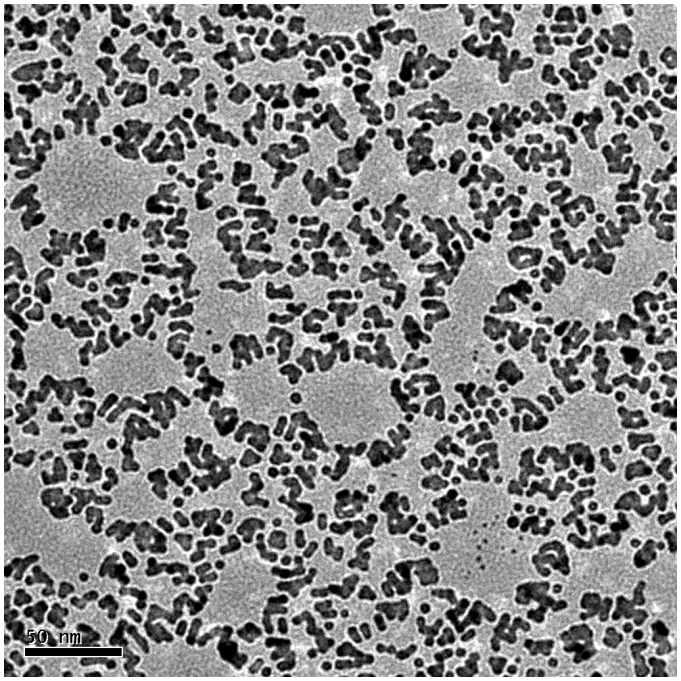

Fig 27(c):
Plasma : 20W RF power
Exposure time:20sec
Area %: 37.4%
Feature count: 369
Magnification: 49000X

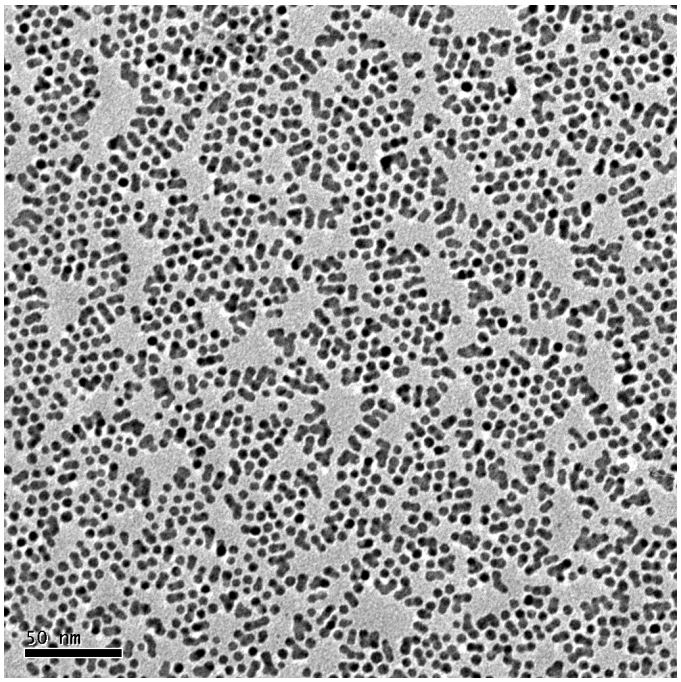

Fig 27(d):
Plasma : 20W RF power
Exposure time:15sec
Area %: 37.7%
Feature count: 1256
Magnification: 49000X

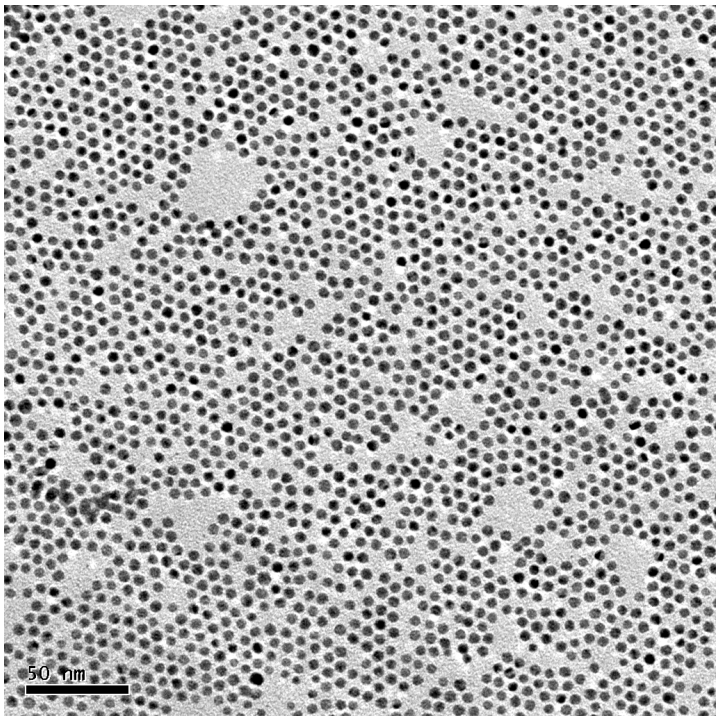

Fig 27(e):
Plasma : 20W RF power
Exposure time:10sec
Area %: 33.6%
Feature count: 1968
Magnification: 49000X

Figure 27: TEM images of 5nm nominal size range particle arrays subjected to different plasma conditions.

The images clearly show a decreasing trend in the extent of coalescence with decreasing time which is as expected. This indicates that the number of particles coalescing is decreasing with decrease in exposure time. Interestingly for 20 seconds exposure time, the nanoparticles were seen coalescing in the TEM chamber itself under the influence of energy provided by the electron beam(fig 20).

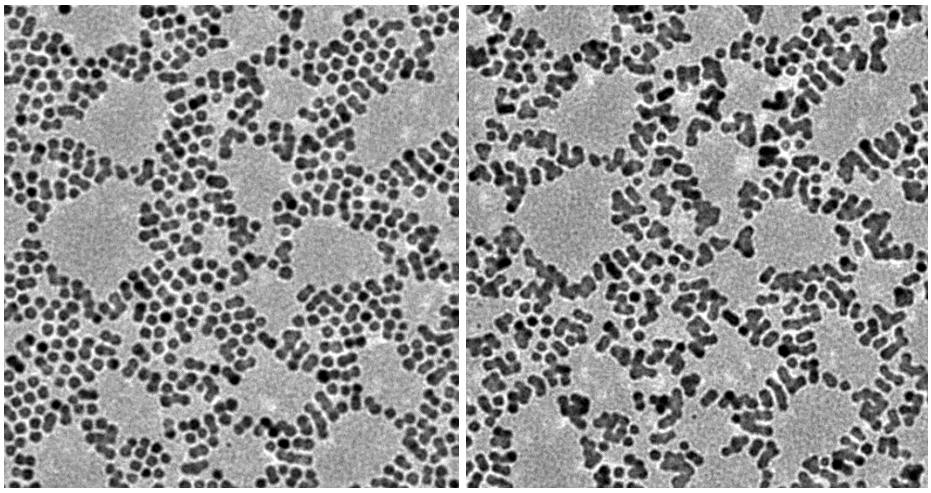

Figure 28 TEM images [20W, 20sec exposure] seen coalescing within a fraction of minute, both at 25K magnification

This implies particles are actually on the verge of coalescence after treatment for 20 seconds and the electron energy was enough to make them coalesce. As seen in the TEM images for 10 seconds case almost no coalescence is observed. In order to quantify the amount of coalescence, the ratio of the number of features before and after plasma treatment for various experiment conditions was calculated and plotted in the figure 21. The data shown is for TEM images captured at 25000X. It is also worth mentioning that in many TEM images there are empty holes having no particles. To account for these and to bring uniformity in the analysis, feature count was scaled according to % of area covered. This assumption is valid if the particles do not form a 3D superstructures(as verified by the negligible change in % of area covered before and after treatment). Although a crude assumption, it gives a good idea regarding the extent of coalescence. From figure## it is seen that the threshold of exposure time, which does not cause coalescence of nanoparticles lies between 10 and 15 seconds for 20W RF power.

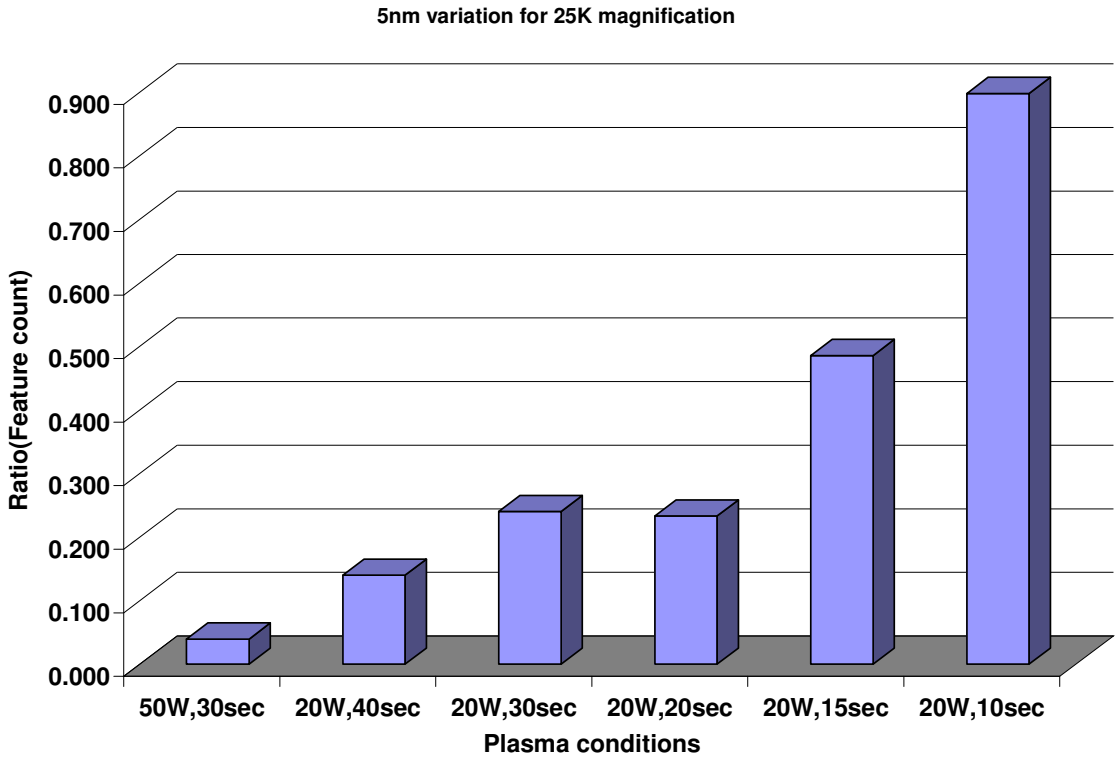

Figure 29: Variation of feature size for 5nm particle size array with experimental condition

Similar study was conducted with nominally 10nm size nanoparticle arrays. It was observed that at low power(10W, 20sec exposure time) there is hardly any change in the array structure. Further studies were conducted with increased power(50W) and exposure time was varied. The TEM images are shown in fig. 22.

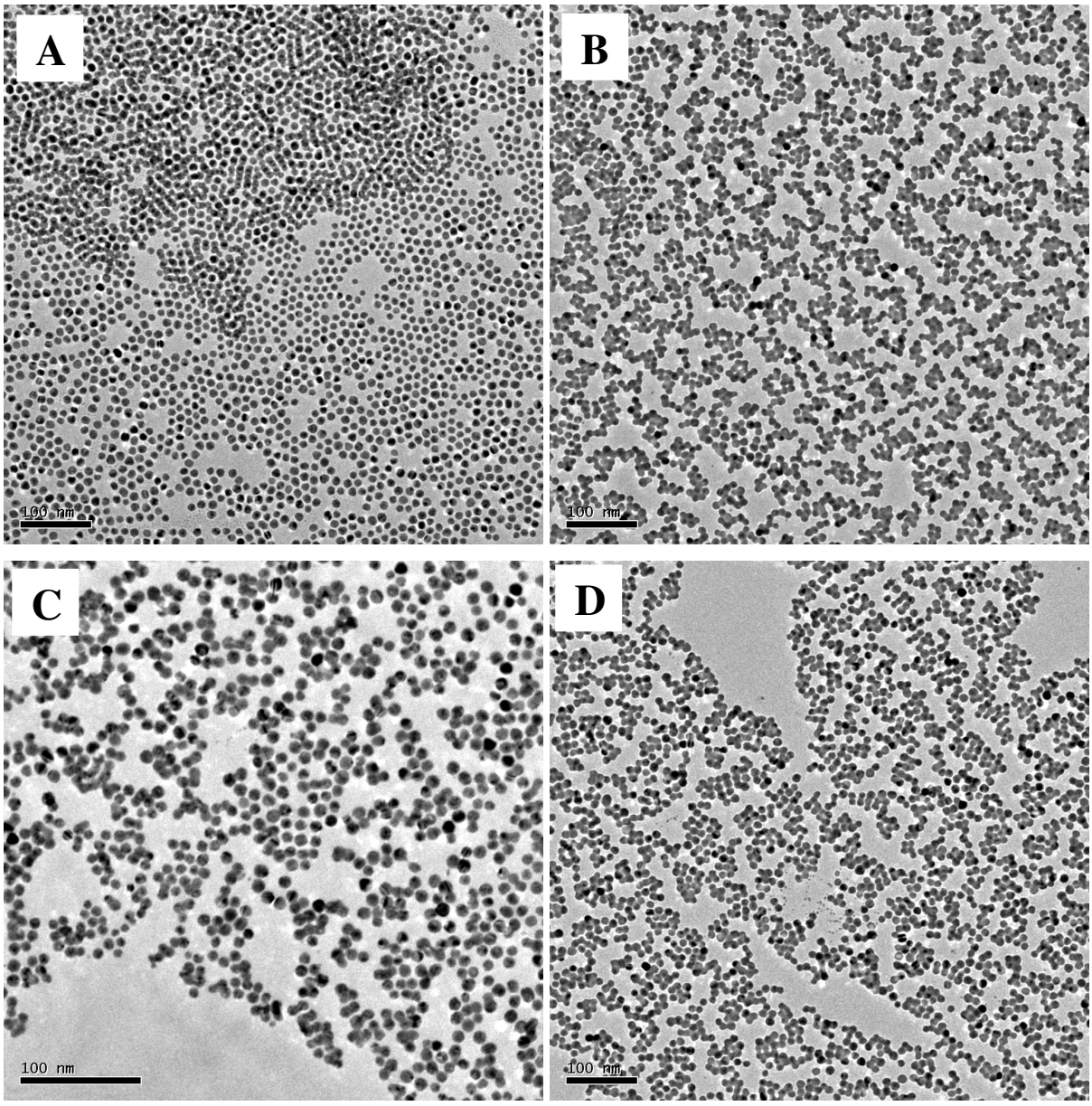

Figure 30: TEM image after Plasma treatment for 10nm nominal size particle. (A).Plasma power: 10W, Exposure time:20sec, 25000X; (B).Plasma power: 50W, Exposure time:30sec, 25000X; (C). Plasma power : 50W, Exposure time:15sec, 39000X; (D). Plasma power : 50W, Exposure time:10sec, 25000X;

As observed in the figures, the particles are unaffected by 20 seconds exposure to 10W plasma but at 50W, even 10 seconds of exposure affects their organization. For 50W power, with 10 seconds exposure time the plasma was seen to have localized effects i.e. patches were seen in which no plasma effect could be discerned. This may be due to the non-uniformity of the plasma treatment or due to some localized shape variation of TEM grid. The feature size variation is shown in figure 22 which indicates that at 50W 10sec, the number of features is almost similar to that prior to plasma treatment. Further studies are required to converge to an optimized exposure time.

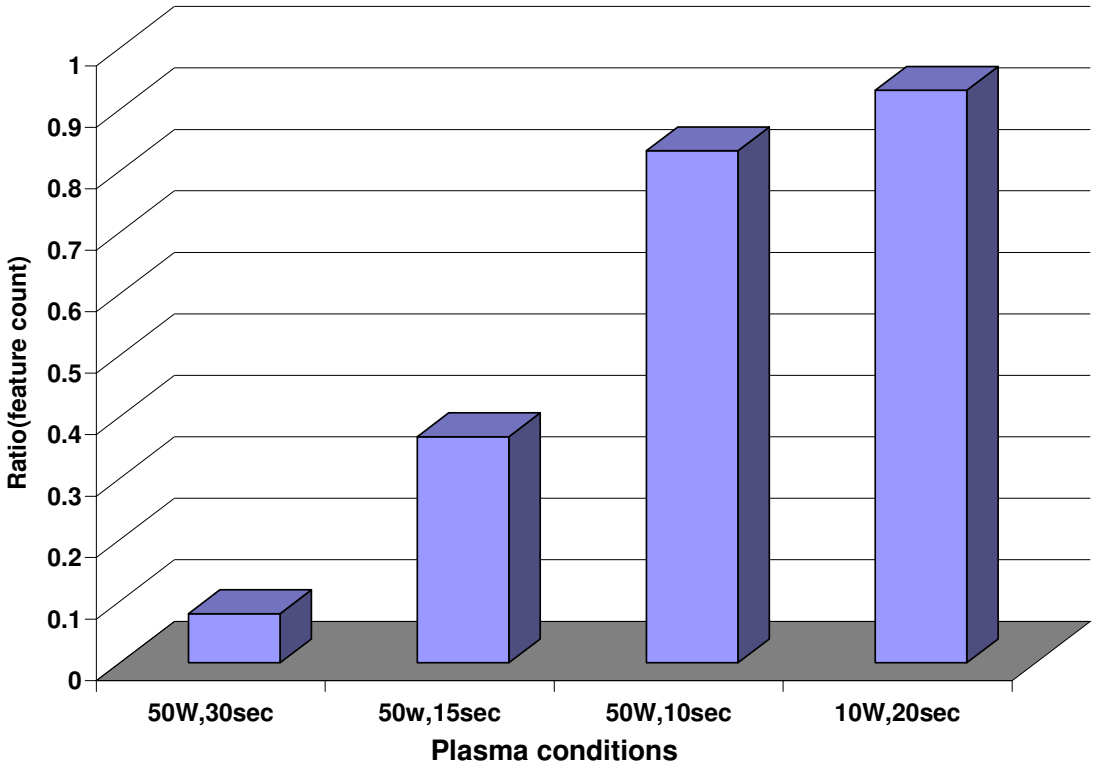

Figure 31: Effect of different plasma treatment conditions on 10 nm size range nanoparticle array

4.3.2 Contact Angle

As discussed earlier, the contact angle of a surface provides the information regarding the hydrophobicity of the surface. Arrays stamped over quartz sample were subjected to the plasma treatment conditions identified by the TEM analysis to be optimum for ligand removal. Contact angle of the array surface before and after plasma treatment are

summarized in table 10. As observed, the contact angle of array is much higher than plain quartz and comparable to the reported data of water on DDT SAMs(115^{o}). After plasma treatment, the contact angle decreases appreciably indicating the decrease in the hydrophobicity of the surface. This can only be due to decrease in area of exposed DDT and an increase in the gold/quartz surfaces(having lower contact angle). TEM studies hint that at the optimized conditions, there is very little lateral movement/coalescence of gold nanoparticles, and so, these results indicate that DDT molecules have been removed(at least from the top surface of the array). The presence or absence of DDT molecules in between the nanoparticles can only be determined if energy filtered TEM images are obtained. This is proposed to be carried out in future.

S.No.	Experiment details	Plasma Conditions (Power, Exposure time)	Contact angle(^{o})	
			Before Plasma	After Plasma
1.	Plain Quartz surface	--	33±3.0	--
2.	Array(5nm size range)	20W, 15sec	84±3.5	47±2.9
3.	Array(5nm size range)	20W, 20sec	96±3.4	65±3.5
4.	Array(10nm size range)	50W,10sec	88±7.6	60±6.9

Table 10: Contact angle data for arrays before and after plasma treatment

4.3.3 UV-Vis and FTIR Spectroscopy

UV-Vis and FTIR of 5nm and 10nm size range MPN arrays before and after plasma treatment was measured. The optimum conditions for plasma treatment, as obtained from TEM analysis, i.e, 20W, 15 seconds for 5nm while 50W, 10sec for 10nm size range MPN arrays were used. UV-Vis spectra shows a peak around 565nm for 5nm size range MPN arrays, while around 580nm for 10nm size range MPN arrays. The red shift with respect to colloidal solution is due to the interparticle distances in MPN array which results in stronger dipole coupling of nanoparticles. There is negligible change in UV-Vis spectra before and after plasma treatment at optimized conditions. Also, the spectra were very much dependent on the orientation of the sample in the UV-Vis chamber. This was because the array was not uniform and if the beam passes through a point where there is poor coverage, the absorbance changes. This was observed in the case of 10nm size range MPN array samples also.

FTIR provides information regarding the presence of DDT molecules[8] based on methylene stretching bands at 2920cm^{-1}. The FTIR spectra are shown in figure 24. It is seen that the characteristic stretching mode of (–CH_2) group is present in all the spectra, indicating the presence of dodecanethiol in all samples. Quantitative comparisons are hindered by the fact that the % coverage of MPN array over the length scales of centimeter in these samples is non-uniform. Further refinement in array fabrication protocols are needed to rectify this situation.

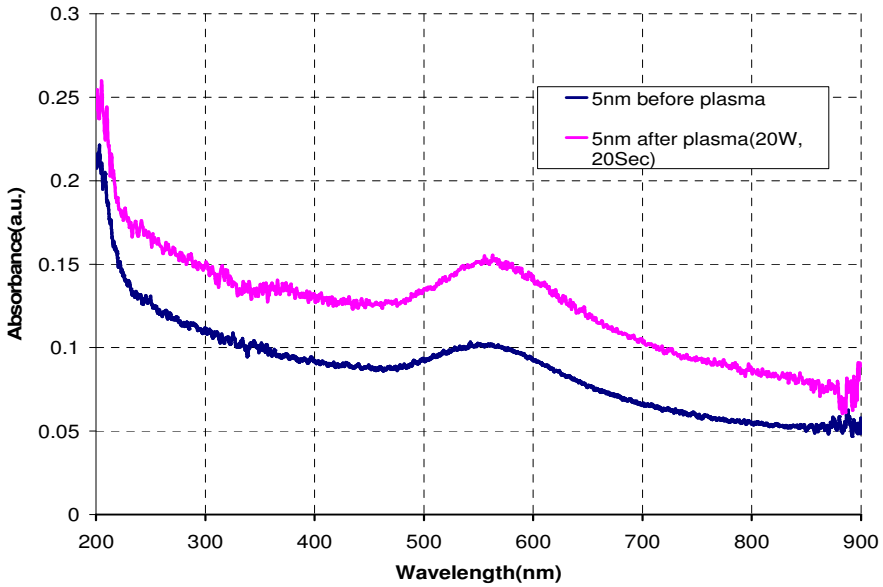

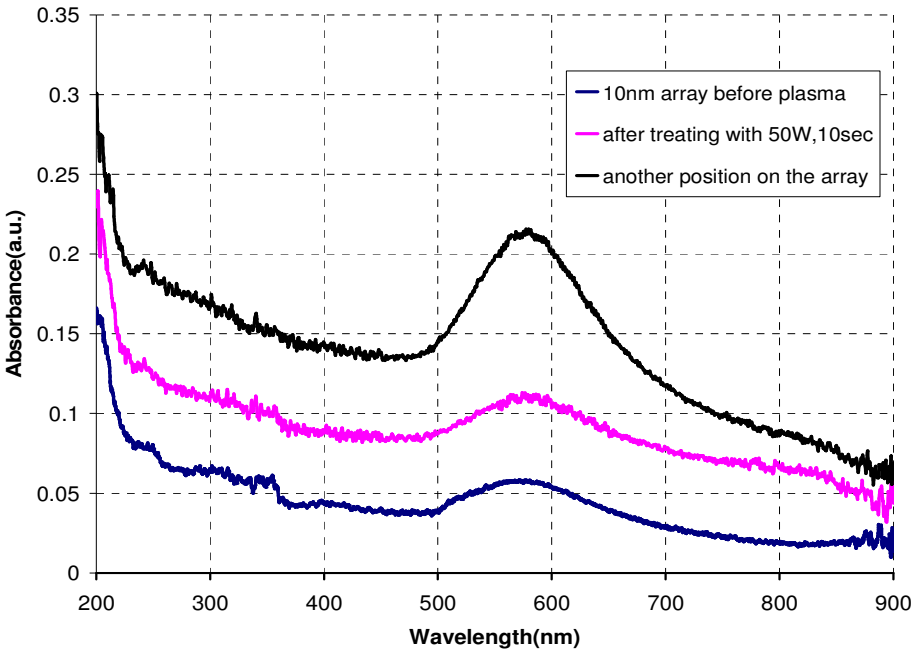

Figure 32 UV Vis of 5nm size range (Above) and 10nm size range(below) particles

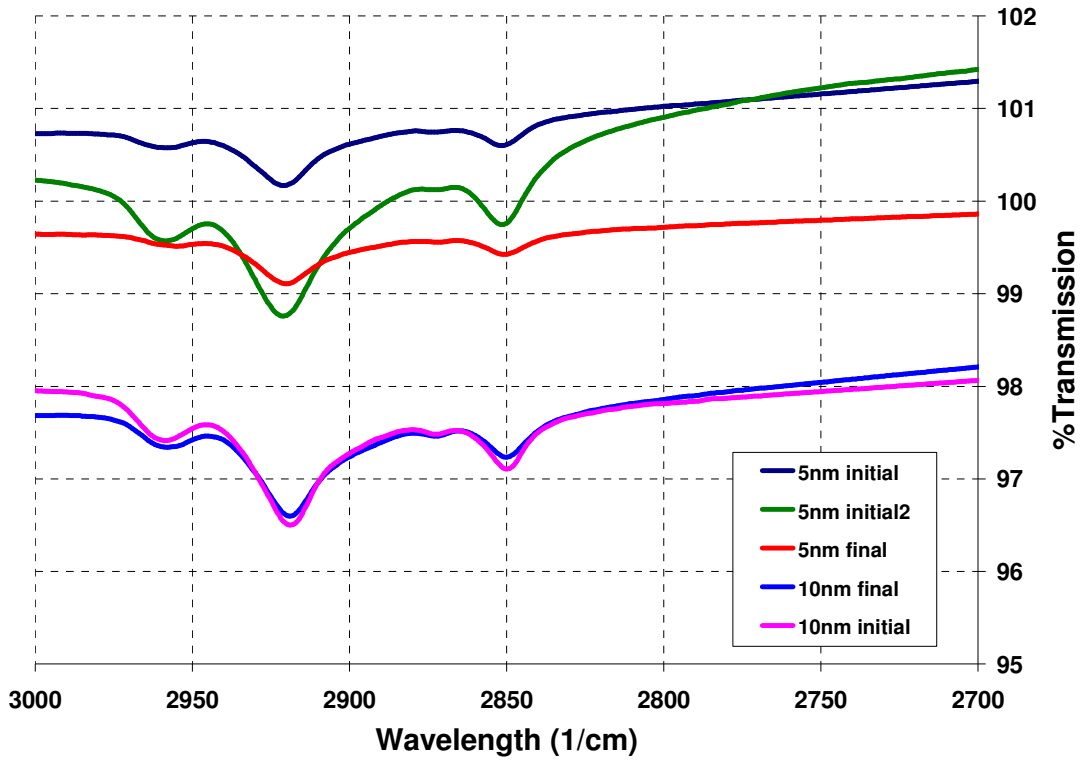

Figure 33 FTIR of the 5nm and 10nm size particle arrays stamped over quartz substrate

4.4 Conclusions

MPN arrays were subjected to different plasma treatment conditions and results presented. Based on the TEM image analysis, the optimum plasma treatment condition for removing the ligands without disturbing the order of the arrays is found to be 20W RF power, exposure time of 10-15 seconds for nominally 5nm size arrays, while it is 50W RF power and 10 seconds exposure time for nominally 10nm size range particles. These conditions are valid for MPN arrays on a smooth, amorphous carbon film(TEM grid). The results may vary for other substrates and need to be addressed in future. Contact angle measurements on MPN arrays stamped over a quartz substrate show a reduction in the contact angle which in turn indicates a decrease in the hydrophobicity of the surface

indicating a loss in dodecanethiol coating. UV-Vis and FTIR studies though useful, were more or less inconclusive due to the lack of uniformity of MPN arrays over large length scales(cm). Different places give different absorbance and it is not easy to keep the substrate in the same position again unless we have a suitable sample holder. Also, as seen in few of the TEM images, the plasma power is not distributed uniformly and there are places where particles have coalesced and places where they haven't in case of lesser time of exposure.

References

[1] Hannon,J.B.; Kodambaka,S.; Ross,F.M.; Tromp,M.; *'The influence of the surface mifgration of gold on the growth of silicon nanowires'*, Nature, **440**, 69-71(2006)

[2] Schmidt,V.; Gosele,U.; *'How nanowires grow'*, Science, **316**, 698-699(2007)

[3] Wu, Y.; Yang, P.; *'Direct Observation of Vapor-Liquid-Solid Nanowire growth'*, J. Am. Chem.Soc., **123**, 3165-3166(2001)

[4] Glass,R.; Moller,M.; Spatz,J.P.; *'Block copolymer micelle nanolothigraphy'*, Nanotechnology, **14**, 1153-1160(2003)

[5] Advanced Plasma Cleaning System, Product Info, available at *http://www.gatan.com/pdf/solarus.pdf* accessed on 12.05.2007

[6] *http://en.wikipedia.org/wiki/Plasma_%28physics%29* accessed on 22.05.2007

[7] *http://en.wikipedia.org/wiki/Contact_angle* accessed on 05.06.2007

[8] Venugopal, S., *'Fabrication of Nanoelectronic Devices using Self-Assembled 2D Arrays of monolayer protected clusters'*, **PhD thesis**, Purdue University(2002)

Chapter 5: Conclusions and Scope for Future Work

Fabrication of bare gold nanoparticle arrays was the focus of this study. Synthesis of gold nanoparticle, fabrication of MPN arrays using self assembly over water surface, and subsequent removal of protective ligand covering was achieved. Plasma etching as a mode of removal of DDT layers from gold nanoparticle was studied and conditions to achieve this for nominally 5 and 10nm MPN arrays were optimized. Some major conclusions of this work are listed below.

- A standard and reproducible protocol for making nanoparticle of the size range 5 and 10 nm was identified. Tannic acid, which may cause problems in array fabrication process, was removed using peroxide and the optimum concentration to achieve this was identified.
- Different cells for array fabrication process were designed and fabricated. It was concluded that array fabrication was best for cell design CD1.
- The optimum plasma treatment condition for removing the ligands without disturbing the order of the arrays is found to be 20W RF power, exposure time of 10-15 seconds for nominally 5nm size arrays, while it is 50W RF power and 10 seconds exposure time for nominally 10nm size range particles.

A better estimate of the concentrations of nanoparticle in the solvent used for making arrays can be obtained if while capping the aqueous solution with DDT, the solution is transferred to centrifuge tubes soon after mixing the reactants. This will ensure that the concentration is uniformly distributed in all tubes. Another way to overcome this problem is to cap smaller volumes of aqueous solution which can be utilized fully in one experiment. Size selective precipitation can be used to obtain a more monodisperse particle size distribution, which will in turn lead to formation of better arrays. Analysis of TEM images was done and the % of covered area reported. A better quantification method for the details in TEM images needs to be identified. The manual way of identifying the right curvature is crude and although reproducible, needs to be standardized. Loss of nanoparticle to the Teflon walls is a matter of

concern(nearly 80% is lost to the walls) and we tried to address the issue by modifying the design of the cell used to fabricate the arrays. Further modifications can be incorporated in the cell design to alleviate this problem. It was also observed that the FTIR and UV-Vis of the arrays stamped over Quartz substrate are not uniform and change with position. A better way to take these measurements such that the beam position does not change in each experiment needs to be identified.

Appendices

Appendix-I: Synthesis protocol for gold nanoparticle

For synthesizing 5nm size range nanoparticles, the procedure adopted is as follows.

1. 79ml of deionized water was taken in an Erlenmeyer flask and heated to 60^{o}C and maintained at that temperature. 1ml 1%(w/v) $HAuCl_4$ solution was added to this.
2. In a 50ml glass beaker, 3ml 1%(w/v) TA solution and 4ml 1%(w/v) sodium citrate solution was added. 10ml DI water was added. Progressively, 0.1ml 25mmol potassium carbonate solution was added until the pH as measured by the pH paper reached in the range of 7.5-8.0. Normally 0.3ml solution is sufficient. The solution was made up to 20ml by adding DI water. This solution is also brought to a temperature of 60^{o}C.
3. Both solutions are mixed and the temperature of the mixture was maintained at 60^{o}C for 15minutes. Constant stirring was continued during the experiment till the end. The colour of the mixture changed within two seconds from pale yellow to wine red. After 15minutes, the solution was heated to boiling and boiled for ten minutes. 1ml hydrogen peroxide solution(30% w/v) was added to this and the solution was again boiled for 10 minutes. Then it was cooled with ice cold water.

For synthesizing 10nm size range particles, the procedure followed is the same except that the amount of TA used is 0.1ml, no potassium carbonate solution was required to be added, and 0.1ml hydrogen peroxide solution was used. Also, the colour of the solution changed slowly so the solution was maintained at a temperature of 60^{o}C for 45 minutes instead of 15minutes.

Appendix-II: Characterization techniques: An Introduction

1. UV-VIS Spectroscopy:

UV-vis spectroscopy is the measurement of the wavelength and intensity of absorption of near-ultraviolet and visible light by a sample. Ultraviolet and visible light are energetic enough to promote outer electrons to higher energy levels. UV-vis spectroscopy is usually applied to molecules and inorganic ions or complexes in solution.

The light source is usually a hydrogen or deuterium lamp for UV measurements and a tungsten lamp for visible measurements. The wavelengths of these continuous light sources are selected with a wavelength separator such as a prism or grating monochromator. Spectra are obtained by scanning the wavelength separator and quantitative measurements can be made from a spectrum or at a single wavelength.

Schematic of a UV-Vis spectrophotometer

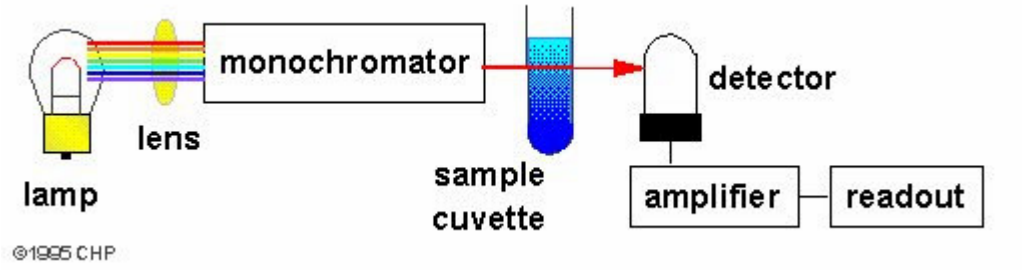

2. Dynamic light scattering(DLS) instrument:

DLS utilizes the Brownian motion of particles to calculate the diffusion coefficient of the particles and back calculates the diameter based on the diffusion coefficient. A monochromatic and coherent LASER light beam is used to illuminate the sample kept in a cuvette and the light scattered by particles is measured at an angle (typically 90^{o}C). The decay of autocorrelation function of the scattered intensity is interpreted in terms of average particle size and polydispersity index by various methods like method of Cumulants, non-negative least square (NNLS). A schematic of the setup of DLS is shown in fig A2.

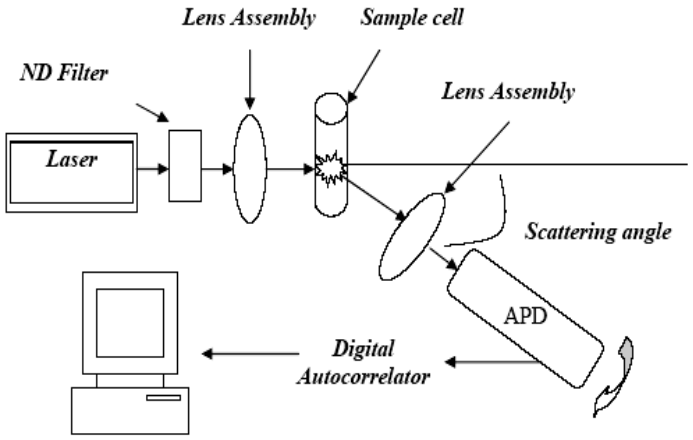

Fig. A-2: Schematic representation of DLS set-up

The setup used for the present work has He-Ne laser source(Melles Griot 75 mW;632.8 nm), which is followed by neutral density filter for varying the power of the beam and a lens assembly which focuses the beam onto the sample cell assembly. The sample contained in a sample cell is surrounded by an index matching fluid(Decahydronaphthalene) filled in a cylindrical vessel. The scattered light from the sample cell assembly is detected with the help of an array of photodiodes. The scattered light intensity flucutations are fed into a digital auto-correlator which generates an autocorrelation function. This autocorrelation function is utilized by various in-built packages to estimate the particle size distribution and polydispersity. Dynamic Light Scattering (DLS) instrument [Model BI-200SM] from Brookhaven Co., with BI-9000AT correlator system was used for obtaining autocorrelation function with software packages NNLS and CONTIN. Usually, six measurements were taken and mean of peak as well as half width was calculated. In few cases, when the distribution of the nanoparticle was very less, or monodisperse nanoparticles, the polydispersity was taken as that reported by the method of cumulants since it gives the best fit for monodisperse nanoparticles.

3. Transmission Electron Microscopy (TEM)

Transmission Electron Microscopy, is a powerful analytical tool for studies in the sub micron to nm range. The basic difference between a TEM and normal microscope is that it uses electrons as the light source instead of normal light. The lower wavelength of

accelerated electrons(6pm at 200kV) makes it possible to get a resolution thousand times better than with a light microscope.

TECNAI G^2(Model F-30) was used for the getting TEM images. A schematic of general TEM is shown in fig A3. The whole chamber is maintained at a low vacuum. Electrons are generated through a Field Emission gun and accelerated. There is a series of electromagnetic lenses, which focuses the electrons on the sample. The focus and magnification can be changed just by changing the current in the lenses. Depending on the nature of sample electrons may get transzsmitted or reflected back. The places where electrons are observed on the screen get illuminated while darker regions are observed for remaining paces. A CCD camera was used to capture the images.

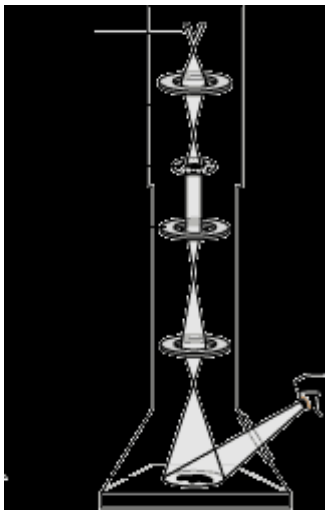

4. AFM: Atomic force microscopy

Atomic force microscopy is a powerful tool to observe topographical features at nano and micron scale. It belongs to the family of scanning probe microscopy in which a probe scans the surface and records the height variation along the path of the movement. Fig A4 shows a schematic of the working principle of the AFM.

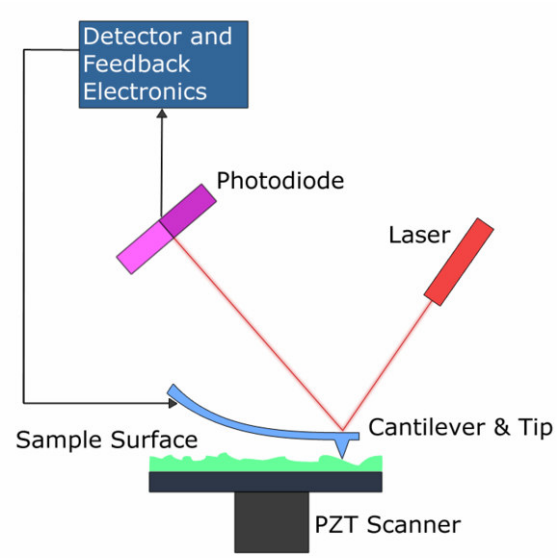

The three important parts of AFM are the controller(detector and feedback electronics), the tip and the PZT scanner. The detector detects the tip orientation and height based on the reflection of a laser light from the tip surface and sends the feedback to the PZT scanner which adjusts the different parameters accordingly. The instrument used in the present study was from Asylum research(Model MFP 3D). There are three different modes of operation of AFM- contact, non-contact and tapping. In its repulsive "contact" mode, the instrument lightly touches a tip to the sample. As it moves over the sample, the vertical deflection of the cantilever, which indicates the local sample height is measured. Thus, in contact mode the AFM measures hard-sphere repulsion forces between the tip and sample.

In noncontact mode, the AFM derives topographic images from measurements of attractive forces without touching the sample. The tip oscillates in its resonant frequency with some set amplitude. The amplitude of the oscillation changes due to the topography of the surface. The height is adjusted so as to keep the amplitude constant and is measured. In tapping mode, tip is in intermittent contact with the surface. This mode is actually a combination of both contact and non contact mode. The controller moves the tip depending on the amplitude.

Appendix-III: Calculations

1. DDT capping requirement

concentration taken	1% in HAuCl4.3H2O	
volume taken	1 ml	
implies	0.01 g	
implies	0.01/393.83 moles =	2.53917E-05
implies	(6.023e23* # of moles) atoms	
Initial # of atoms in the solution =	1.52934E+19	
for 10 nm size particles		
% at the surface	15.3	
total # of atoms on surface =	2.33989E+18	
# of thiols at the surface =	1/6th of the total surface atoms	
which is =	7.79963E+17	
moles of thiol required =	1.29497E-06	
molecular wt of thiol =	202.4 g/mol	
wt of thiol required =	0.000262103	
density =	0.845 g/ml	
ml of thiol required =	3.10E-04	
no of particles formed	7.23879E+14	
per ml	9.04849E+12	
	0.16 microlit	
for 5 nm size particles		
% at the surface	28.3	
total # of atoms on surface =	4.32803E+18	
# of thiols at the surface =	1/6th of the total surface atoms	
which is =	1.44268E+18	
moles of thiol required =	2.39528E-06	
molecular wt of thiol =	202.4 g/mol	
wt of thiol required =	0.000484805	
density =	0.845 g/ml	
ml of thiol required =	0.000573733	
	0.3 microlit	

2. Ideal Coverage area

Assuming an hexagonally packed 2D array with particles of diameter "d"
The repetitive unit consists of a three particles touching each other with centres forming a equilateral triangle of side 'd'
# of particles in the triangle = ½ {3 *1/6}
area contribution = (½*pi*d^2)*1/2
triangle area = ½ *d^2 *(sqrt(3))/2
filled area = the area contributed by particles/area of the triangle formed

= 90.7%

since in our case the particles are actually separated by DDT layer hence the area covered can be found by replacing ‘d’ by ‘d-t’ where t is the distance between the two particles.

From table , the ideal distance for 5nm size range particles is

2.2 nm(mean value taken)

% coverage ideal = 43.8%

For 10nm size range particles

3.5 nm

% coverage ideal = 49.8%

Appendix-IV: MATLAB code

MATLAB Program to get superimposed images with centroids.

```
clear all,close all,imtool close all
I1=imread('20070505as5nm2_2f.jpg');
I2=imread('20070505as5nm2_2f_bdry.jpg');
figure,imshow(I1);
figure,imshow(I2);
for i = 1:1024
   for j=1:1024
      if ( I2(i,j)<10)
         I3(i,j)=0;
      else
         I3(i,j)=I1(i,j);
      end
   end
end
figure,imshow(I3);hold on
I4=dlmread('alokcentroid.txt');
scatter(I4(:,3),I4(:,4),'+','r');
x=(I4(:,3));
y=(I4(:,4));
for i = 1:221
      X(i,1)= x(i);
      X(i,2)= y(i);
   end
```

Appendix-V: Chemicals used and supplier information

1. Hydrogen tetrachloroaurate (lll) hydrate, 99.999 % from Sigma Aldrich
2. 1-Dodecylmercaptan (DDT) ($C_{12}H_{26}S$), 98.5 % from Sigma Aldrich
3. Tannic acid (MW 1701.23) ACS reagent from ACROS ORGANIC
4. Sodium Citrate (MW 294.1) from Sigma Aldrich
5. Oleic acid LR grade from SD-Fine chemicals
6. Poly-Vinyl Pyrrolidone (MW 30,0000) from Sigma Aldrich
7. Sodium Oleate for synthesis from Kemphasol
8. Aurion Gold Sol, gold Particle: 6nm, COV <=15%, from Electron Microscopy Sciences